Lake Elsinore/Canyon Lake TMDL Task Force

Lake Elsinore & Canyon Lake Modeling

Technical Memorandums 2015-16

Michael Anderson, Ph.D.
University of California, Riverside

Technical Memorandum

Task 1.0: Surface Elevation and Salinity in Lake Elsinore: 1916-2014

Objective

The objective of this initial task was to develop and calibrate a 1-D hydrodynamic model for Lake Elsinore to simulate volume, surface elevation and salinity in Lake Elsinore for the period 1916-2014, and compares model-predicted values with available observations.

Approach

The DYRESM model was used to simulate conditions in Lake Elsinore under the 1-D assumption, *i.e.*, that lateral differences in water column properties are small and that the primary gradients in properties occur in the vertical dimension. The 1-D assumption is appropriate given the lake's relatively simple basin shape and the long time horizon of interest. Specifically, this assessment evaluated the time period from 1916-2014 (99 yrs). This time interval was selected because of availability of flow, rainfall and air temperature data for this full period.

Daily flows of the San Jacinto River into Lake Elsinore at USGS gage #11070500 were downloaded from USGS. Daily rainfall records were provided by RCFCD for the Quail Valley, (1958-2014), San Jacinto (1940-2014) and Hemet (1916-1940) rain gauges to estimate runoff from the local 13,340 acre watershed not captured by gaged San Jacinto River flows (Anderson, 2006). The available Quail Valley rainfall data were used for the 1958-2014 period without any correction. Regression equations developed between measured Quail Valley precipitation and that at San Jacinto (r^2=0.70) and Hemet r^2=0.52) were used to predict rainfall at Quail Valley for 1940-1958 and 1916-1940, respectively. Daily average air temperature, relative humidity/vapor pressure, shortwave radiation, and windspeed for 1985-2014 were taken from CIMIS station #057 at UC Riverside. Air temperature records for 1916-1985 were downloaded from the NOAA National Climatic Data Center for the Corona station that provided the longest nearby continuous record. Average shortwave solar radiation, vapor pressure and windspeed from CIMIS station #057 for each calendar day were used for the earlier part of the record when measurements of these meteorological attributes were not available (pre 1985).

The elevation-area data for the natural lake basin was used from the 1916-1995 period (*i.e.*, pre-LEMP), while the current reconfigured basin (*i.e.*, post-LEMP) was used for the period 1996-2014. A 10-minute time-step was used for the simulations.

Meteorological and Flow Records

Analysis of meteorological and flow data over the past 99 years highlights the inter-annual variability present in the region. Annual rainfall within the local watershed of Lake Elsinore ranged from 2.04 inches in 2006 (based on water year) to 26.97 inches in 1977 (Fig. 1). Precipitation averaged 10.1 inches over this period, while the median was 8.89 inches. As suggested in Fig. 1, precipitation was not normally-distributed about the mean value; precipitation was found to be log-normally distributed however (mean log rainfall 0.96±0.21).

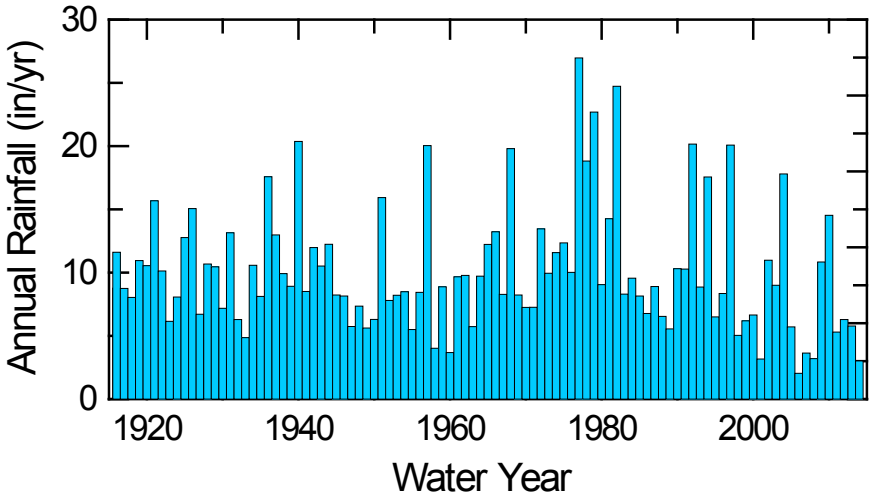

Fig. 1. Annual rainfall to local watershed adjacent to Lake Elsinore.

The mean annual air temperature has also varied over the past 99 years (Fig. 2). Temperature has averaged 17.08±0.81 °C over this interval, with a minimum value of 15.4 in 1934 and a maximum temperature of 19.5 °C in 1984, with a statistically significant increase ($p<0.001$) in average annual air temperature at a mean rate of 0.016°C/yr, or an increase of almost 1.6°C over the study period. This rate of change is larger than the global mean surface temperature increase of approximately 1.0°C over this same time period.

Annual runoff to Lake Elsinore measured at the USGS gage exhibited even more dramatic variation (Fig. 3). There were 5 years where virtually no flow was recorded at the gage, and 25% of the time, annual flow was <100 AF/yr. At the other end of the spectrum, 22 years were found to have flows >10,000 AF/yr, supporting the general notion of an El Nino-type event on average every 4-5 years. Low flows are difficult to see on this figure due to the periodic very large flows (e.g., water years 1916 and 1980).

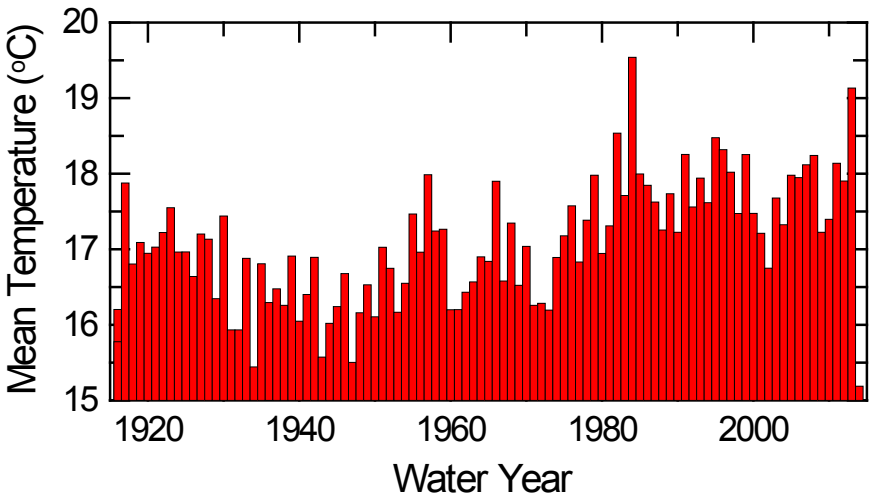

Fig. 2. Mean annual temperature at Corona (NOAA)

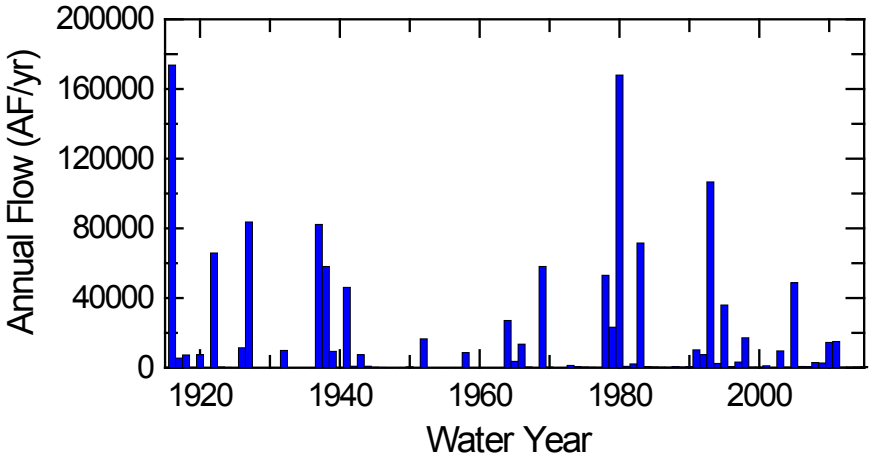

Fig. 3. Annual flow at USGS gage #11070500 (San Jacinto River near Lake Elsinore)

Local rainfall values (Fig. 1) were used to estimate local runoff flows to the lake (i.e., runoff from the land areas surrounding the lake and not captured by the USGS gage) (Fig. 4, orange bars). Previous measurements at the lake suggested a local runoff coefficient of about 0.3, or about 30% of precipitation contributed to runoff (Anderson, 2006), while 70% was on average retained by the soil through infiltration and storage within the porosity of the soil and weathered bedrock. Since runoff in urban and suburban-type watersheds is strongly influenced by the amount of impermeable surfaces (roads, parking lots, driveways and rooftops), an assumption was made that the runoff coefficient measured a few years ago adequately reflects current levels of development, but that the runoff coefficient would likely have been lower earlier in the study period. Specifically, a runoff coefficient of 0.2 was assumed from 1916-1960, 0.25 for 1961-

1980, and 0.3 for 1981-present. Local runoff averaged 2813 AF/yr. Recycled water was also recently added over a number of years (Fig. 4, green bars).

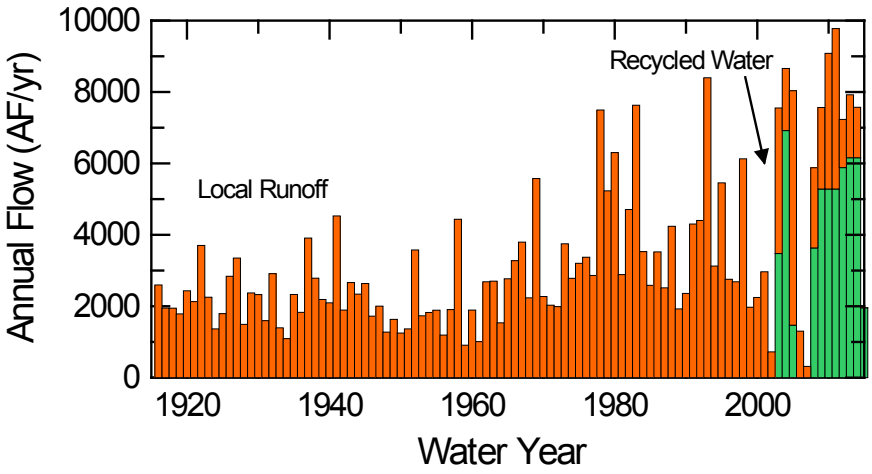

Fig. 4. Annual flows to Lake Elsinore due to local runoff (orange bars) estimated from precipitation and runoff coefficient and recycled water additions (green bars).

Model Calibration: 1964-2014

Lake Level

Daily average values for meteorological parameters were used in conjunction with daily flow data to predict volume, surface elevation, and salinity in Lake Elsinore over time. Lake surface elevation has been recorded regularly by Elsinore Valley Municipal Water District staff since 1964, following the dry lake bed from approximately 1954-1964 and beginning with importation and delivery of Colorado River Aqueduct water. Recorded lake level data were provided by Jesus Gastelum and used to calibrate the model with respect to the water budget.

Preliminary simulations used January 1, 1964 as the starting point with the introduction of Colorado River water beginning on February1, 1964 with model default parameter values; the model was found to over-predict water levels and surface water temperatures. More detailed analysis indicated that the model was under-predicting evaporation when compared with theoretical ET_0 values measured at UCR CIMIS station #057. This appears to be due to use of daily average values for air temperature, vapor pressure and windspeed, which do not adequately reflect the warm dry afternoon winds that result in much of the evaporative heat flux and water loss that occurs at the lake. To account for this, the bulk aerodynamic transport coefficient was lowered from 1.3×10^{-3} to 0.3×10^{-3} and non-neutral atmospheric stability was assumed; this was found to yield an annual evaporation rate from the lake that matched the rate of 1.47 m/yr reported at the UCR CIMIS station. Using these parameter values, predicted lake surface elevations from simulations matched much more closely measured values over the 1964-2014 period, except immediately following a large runoff event that dramatically

increased lake level and wetted lake area. This discrepancy was attributed to rapid infiltration into dry lake bed sediment and surrounding soils and potential groundwater recharge. This was especially evident in 1964 when water was introduced in the lake basin following an approximately decade-long dry lake bed, and in 1970 and 1980 when large volumes of runoff was delivered to the lake (Fig. 3). Following the major runoff event in 1980, about 40% of the runoff delivered to the lake was estimated to have saturated soils and recharged groundwater as a result of rewetting more than 2000 acres of the lake's approximately 6000 acre natural basin. Infiltration rates were estimated to be 0.7 cm/d. Subject to these corrections, the model predicted lake surface elevations that very closely followed measured values (Fig. 5). Note that the natural 6000 acre basin was assumed to be in place through 1995, at which time the LEMP project was completed which reduced lake area and increased mean depth.

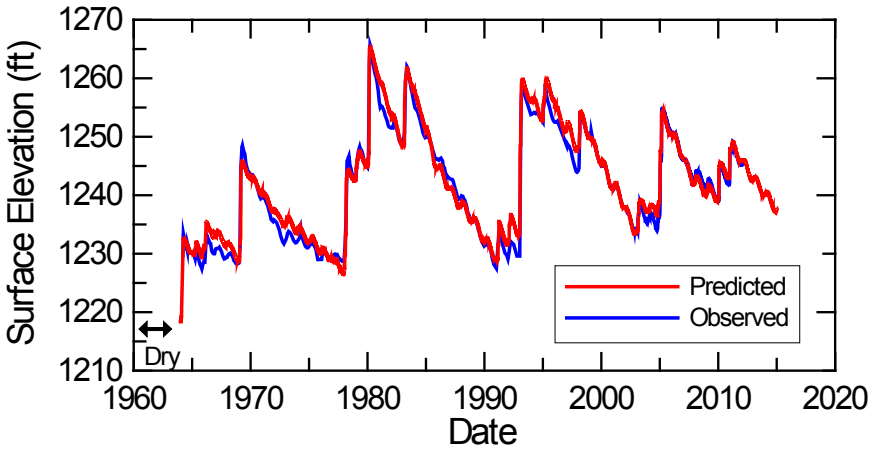

Fig. 5. Surface elevation of Lake Elsinore: 1964-2014 (blue line represents measured values; red line represents predicted values).

The model quite reasonably reproduced lake level in the post-LEMP basin (1996-2014) without any corrections for infiltration so none were applied over this interval (Fig. 5). This is thought to be a result of the tight clay layer present across much of the lower part of the lake basin that limits deep percolation and minimizes loss to unsaturated soil or groundwater. The reconfiguration of the basin as a result of LEMP thus not only reduced evaporative loss but all quite substantially reduced losses to unsaturated soils and groundwater. Root-mean square error (RMSE) of model-predicted surface elevations was 0.0047 ft.

Salinity

Salinity in the lake is a function of runoff volumes, salinities of those flows, and evapoconcentration. Based upon available measurements and reports, average TDS values for the San Jacinto River, local runoff and recycled water were taken as 300, 150 and 700 mg/L. TDS levels would also vary markedly as a result of rewetting of a dry

evaporite lake bed, and during episodes of evapoconcentration as well as large runoff events. The amount of salt deposited during the approach to and subsequent decade-long dessication period of 1954-1964 is not known, but local accounts do report frequent episodes of intense blowing dust and salt. It is likely that wind erosion was a mechanism by which a significant amount of salt was exported from the lake basin. Based upon water budget calculations (Fig. 5) and other factors, initial salinity was varied and model results were compared with observed values. Reasonable agreement was found when initial salinity was set at 7,500 mg/L TDS with a maximum water depth of 18 cm. Importantly, this TDS value was in good agreement with the TDS value of 8,000 mg/L measured in sediment porewater above the clay dessication layer from a core collected from the deepest part of the lake (unpublished data). (The model requires at least 18 cm of water be present in the lake and also requires that the salinity of the water remain below about 42,000 mg/L based upon the UNESCO equation of state for water that governs vapor pressure, specific heat and other thermodynamic properties of water.) The model predicted wide swings in TDS, with extended periods of evapoconcentration and increasing salinity followed by rapid declines as a result of large runoff events (Fig. 6). Model predicted TDS levels were in good overall agreement with measured TDS values available over the past 15 years when studies began in earnest at the lake (Fig. 6). RMSE of model-predicted TDS concentrations was 203 mg/L.

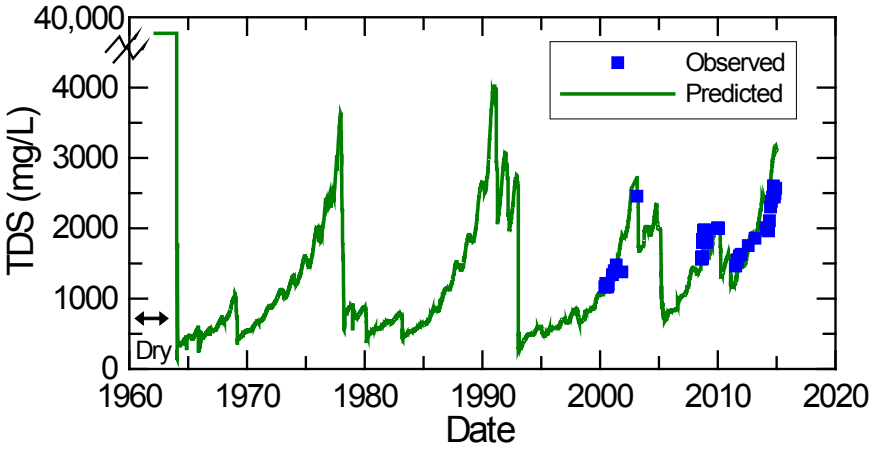

Fig. 6. Total dissolved solids (TDS) concentration in Lake Elsinore: 1964-2014 (blue symbols represents measured values; green line represents predicted values).

The model accurately reproduced measured lake surface elevations (Fig. 5) and also reasonably reproduced measured TDS concentrations (Fig. 6). The model was thus deemed suitable for predicting water balances and salt balances in Lake Elsinore over the longer 1916-2014 time period, and also serves as an appropriate starting point for simulations of water quality over the past century.

1916-2014

The period from 1916-1964 was then simulated and appended to 1964-2014 model results (Fig. 7). The initial condition for the lake on January 1, 1916 was not precisely known, but the average depth of 5 m, temperature of 12°C and TDS of 250 mg/L was assumed based upon historical accounts of lake levels in the late 1930s and 1950s. To account for loss to unsaturated soils and groundwater following large runoff events into the large shallow natural basin, flows were reduced by an average value of 30% based upon detailed water accounting over the 1964-1995 period previously described. The results from 1916-1950's should thus be considered provisional; notwithstanding, this period also demonstrated considerable variation in lake level (Fig. 7).

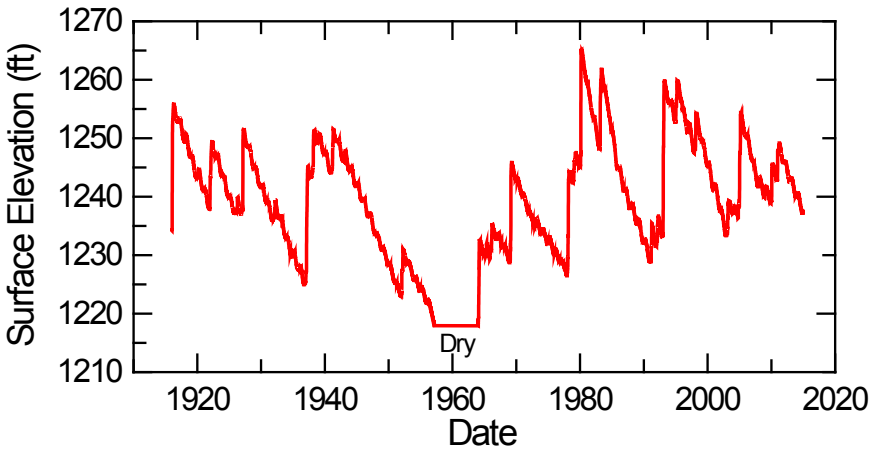

Fig. 7. Model-predicted surface elevations of Lake Elsinore: 1916-2014.

The model predicted low lake levels in 1935, with a minimum surface elevation of 1225.3 ft and depth of 2.3 m in December 1936 before spring rains in 1937 increased lake level to 1245.2 ft and depth of 8.34 m (Fig. 7). Rainfall and runoff the following spring (1938) further increased lake level to 1251.3 ft. The surface area of the lake increased from 1450 to 4895 acres over this time period (Fig. 8). The model predicted the lake level to decline through much of the 1940's, fully dry out by early 1957 and remain essentially dry until February 1964 (Figs. 7, 8). Historical accounts suggest the lake dried out somewhat earlier than that, potentially by 1954 or 1955.

Salinity varied inversely with surface elevation and lake area, with very large increases in TDS present as a result of evapoconcentration at low lake levels (Fig. 9). Values exceeding 3000 mg/L were predicted in the 1930s, 1940s-1964, 1978 and 1990 (Fig. 9). The TDS was predicted to exceed that of seawater upon complete dessication in the late 1950s.

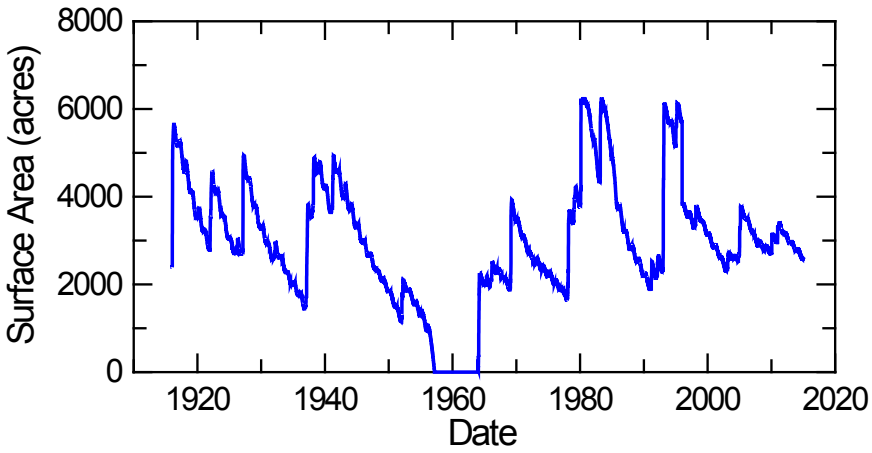

Fig. 8. Model-predicted surface area of Lake Elsinore: 1916-2014.

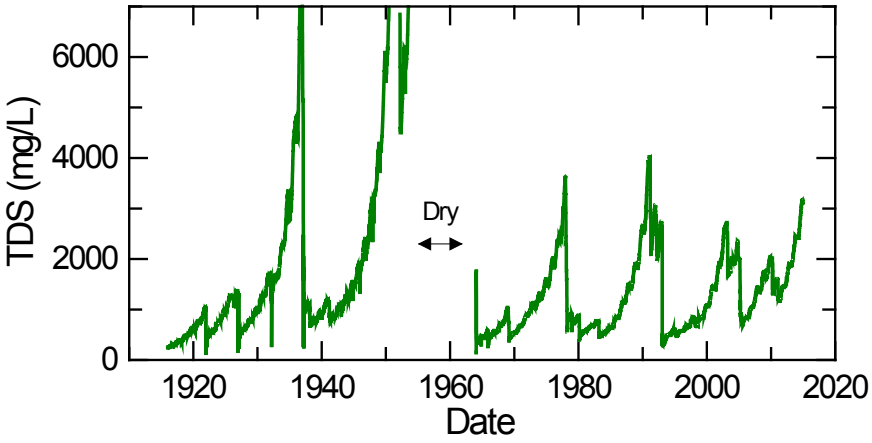

Fig. 9. Model-predicted TDS concentrations in Lake Elsinore: 1916-2014.

The simulation results presented in Fig. 9 can also be used to track salt accumulation within the lake basin. While it is difficult to visually track salinity given the highly dynamic lake level that concentrates and then dilutes the salt load, TDS concentrations at a common surface elevation, and thus also lake volume, provides a straightforward way to estimate of the rate of salt accumulation within the lake. At a constant lake level of 1240 ft, TDS concentration was observed to increase at a rate of 39 mg/L/yr between 1920-1950 (r^2=1.00) for the large shallow natural lake basin (Fig. 10). The rate of salt accumulation at constant elevation was similar for the period 1970-2002 (30 mg/L/yr) even though the post-LEMP data point shifted the slope of the line down somewhat. Most notably, addition of recycled water at rates shown in Fig. 4 approximately quadrupled the rate of salt accumulation, to 136 mg/L/yr (r^2=1.00), despite the smaller deeper (post-LEMP) lake basin that would be expected to reduce the rate of evapoconcentration of salts relative to the natural basin (Fig. 4). This provides the first quantitative estimate of effect of recycled water addition on salt load in Lake Elsinore.

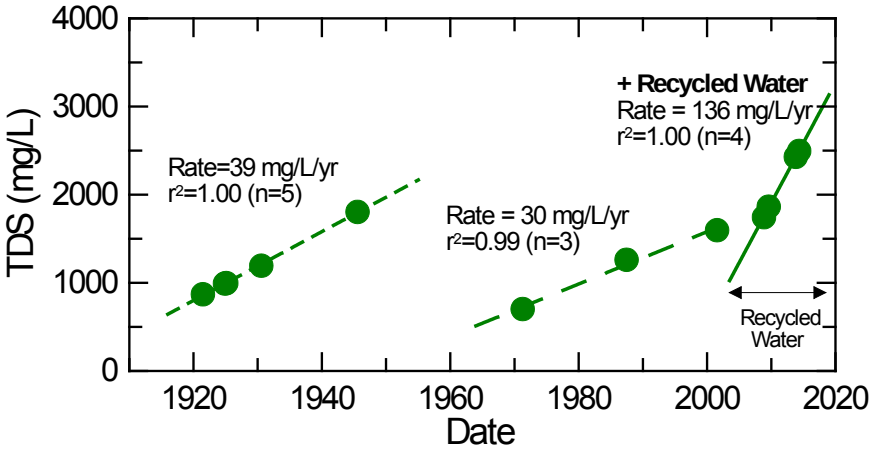

Fig.10. Model-predicted TDS concentrations in Lake Elsinore at constant lake elevation of 1240 ft showing marked increase in rate of salt accumulation since recycled water additions began in late 2002.

Part of the interest in simulating the early part of the past century was to include this longer record in a probabilistic description of the range of conditions in the lake and the frequency of low lake levels and high salinities that would have profoundly negatively affected its beneficial uses. The results from Figs. 7-9 were used to develop cumulative distribution functions that describe the exceedance frequency of a given condition, *e.g.*, frequency over the past 99 years that the lake level was below 1240 ft, or salinity exceeded some critical biological threshold (Fig. 11).

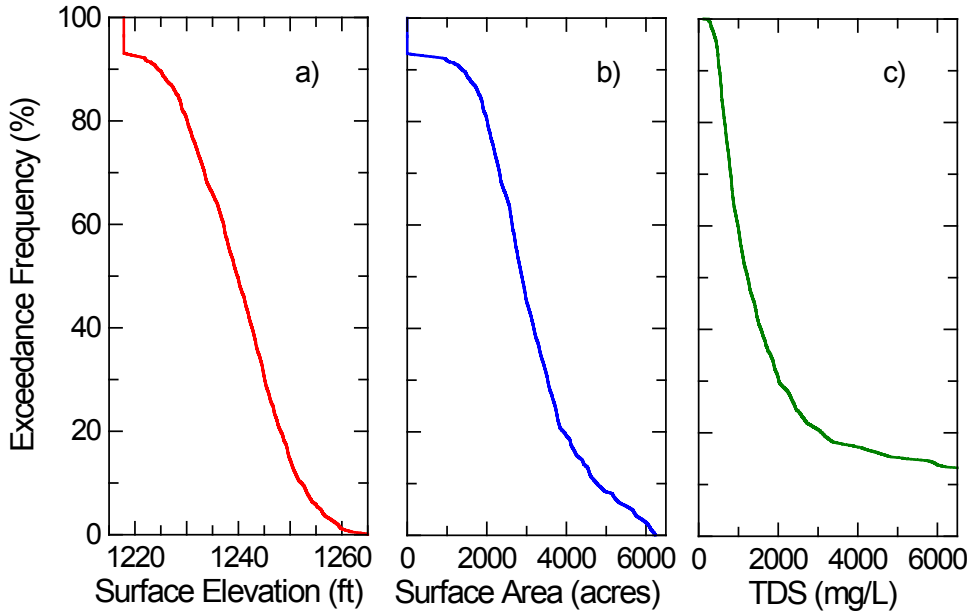

Fig. 11. Exceedance frequencies for a) lake surface elevation, b) lake surface area, and c) TDS concentration.

Based upon model predictions, the lake was dry 6.8 of the past 99 years, with a surface elevation <1218 ft and no wetted surface area (Fig. 11). The frequency of exceeding a given lake elevation and area decreased with increasing values. Selected exceedance frequencies are provided in Table 1. The lake property at an exceedance frequency of 50% corresponds to the median value over the simulated period; thus, the median lake level was at 1239.8 ft, surface area was 2881.4, and TDS was 1232 mg/L (Table 1). Values higher than these were found less frequently, e.g., 5% of the time, the TDS was predicted to exceed that of ocean water (when the lake was essentially dry).

Table 1. Values of surface elevation, area and TDS concentration in Lake Elsinore at selected exceedance frequencies based upon simulations for 1916-2014..

Exceedance Freq (%)	**Elevation (ft)**	**Area (acres)**	**TDS (mg/L)**
90	1224.5	1380.2	524
50	1239.8	2881.4	1232
10	1252.1	4766.7	13,786
5	1255.8	5641.7	>42,000
1	1260.4	6137.6	>42,000

It is worth noting that a 90% exceedance frequency for a lake surface elevation of 1224.5 ft or surface area of 1380.2 acres (Table 1), also corresponds to a 10% frequency of being *less* than these values. Thus using the 99 year record as an index, 10 years out of the past 99 years would yield elevations and areas below these values.

Conclusions

Results from these initial simulations indicate:

(i) the model accurately predicted measured lake surface elevations and available TDS concentrations;

(ii) significant loss of water to unsaturated soil and groundwater occurred in the large shallow natural basin (i.e., pre-LEMP) following large runoff events;

(iii) losses to unsaturated soils and groundwater were not apparent for the reconfigured (post-LEMP) basin;

(iv) over the past 99 years, the model predicts that the lake was dry for 6.8 years, with salinity near or exceeding that of sea water when the lake approached dessication;

(v) salt has accumulated in Lake Elsinore at a predicted rate of 30-39 mg/L/yr at a surface elevation of 1240 ft for much of the past century;

(vi) addition of recycled water has accelerated the predicted rate of salt accumulation at 1240 ft elevation to 136 mg/L/yr since addition of recycled water began in late 2002.

Next Step

The next step will be to simulate Lake Elsinore using the reconfigured (post-LEMP) basin for the entire 1916-2014 period, with and without recycled water additions, to compare effects of recycled water on lake surface elevation, area and salinity. Comparison will also be made with the results reported herein for the natural basin (1916- 1995) and transition to the reconfigured basin (1996-2014).

References

Anderson, M.A. 2006. *Predicted Effects of Restoration Efforts on Water Quality in Lake Elsinore: Model Development and Results.* Final Report to LESJWA. 33 pp.

Technical Memorandum

Task 1.1: Influence of Recycled Water Supplementation on Surface Elevation and Salinity in Lake Elsinore: Model Predictions for 1916-2014 with Current (post-LEMP) Basin

Objective

The objective of this task was to simulate Lake Elsinore using the current (post-LEMP) basin for the entire 1916-2014 period, with and without recycled water additions, to compare effects of recycled water on lake surface elevation, area and salinity.

Approach

The calibrated DYRESM model used in Tech Memo 1.0 that simulated lake level and salinity in Lake Elsinore under conditions present at the lake from 1916-2014 (Anderson, 2015) will be used with the current (post-LEMP) basin. The lake will be simulated (i) assuming San Jacinto River flow and local runoff with TDS concentrations of 300 and 150 mg/L, respectively, and (ii) water supplemented with up to 5000 acre-feet of recycled water with a TDS concentration of 700 mg/L when the lake level drops below 1240 ft. Crest elevation was set to 1255 feet; the model assumes that the discharge capacity when the lake reaches crest elevation is effectively unlimited. All other model parameters will remain unchanged from those described in Tech Memo 1.0. The reader is referred to that document for details.

Results

Runoff from the San Jacinto River and local watershed into Lake Elsinore (with post-LEMP basin) for the 1916-2014 period were predicted to yield wide swings in lake surface elevation (Fig. 1, solid orange line). The model predicted that the lake level would remain above 1240 ft from early 1916 -1931, with water flowing out of the lake in 1916, 1922, and 1927. The water surface elevation decreased to about 1229 ft above MSL in 1936 before rainfall and runoff increased the lake level sufficient for water to again flow out of the lake in 1937 (Fig. 1, orange line). Limited runoff from 1943-1964 failed to meet evaporative losses and resulted in the lake level declining and eventually going dry in 1961-1964. Importantly then, while LEMP has a pronounced benefit helping maintain water level relative to the natural basin (Anderson, 2013), the re-engineered smaller basin is nonetheless unable to maintain water in the lake during periods of prolonged drought (Fig. 1, orange line).

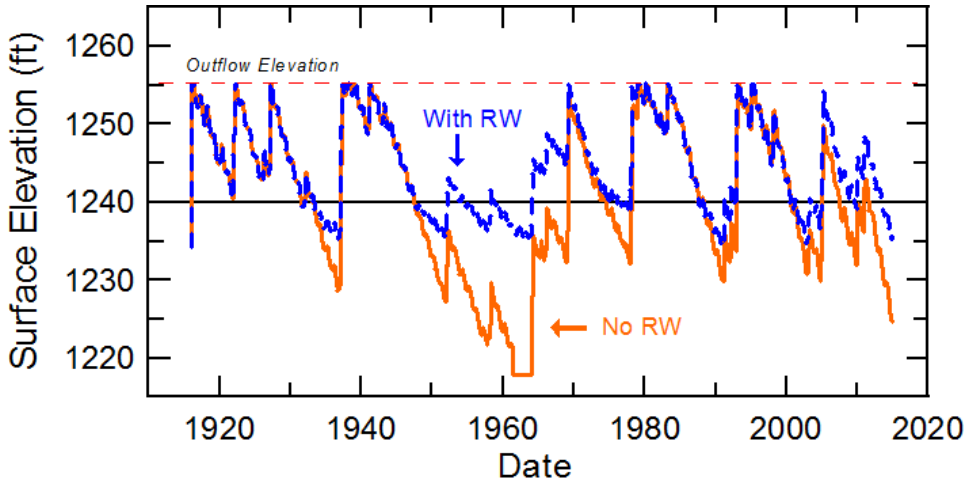

Fig. 1. Lake surface elevation with LEMP basin and natural flows (solid orange line) and supplemented inflows with recycled water (dashed blue line).

Supplementation of natural inflows with recycled water when the lake level declined below 1240 ft helped support higher lake levels and was predicted to maintain surface elevations above 1234.5 ft throughout the entire 99-yr period (Fig.1, dashed blue line). The re-engineered basin together with supplementation with recycled water helps prevent extremely low lake levels.

The increased lake surface elevations resulting from recycled water additions also had a marked effect on lake surface area (Fig. 2).The lake area rarely dropped below 2500 acres (range 2372 – 3844 acres) and averaged 3088 acres with recycled water supplementation. In contrast, a much wider range of surface areas were predicted with natural flows, from 0 acres (i.e., dry lake bed) in early 1960s to 3844 acres (full pool) during strong El Nino events (Fig. 2). The lake averaged 2772 acres over the duration of the simulation. Recycled water additions thus help ensure greater recreational opportunities and provide more substantial habitat when compared with natural inflows only.

The re-engineered basin also resulted in lake surface elevations that periodically reached the crest elevation of 1255 ft, resulting in overflows and some flushing of the lake (Fig. 3). The DYRESM model assumes no limits on outflow rates when surface elevations exceed crest elevation, so the predicted daily outflow rates in many cases exceed the capacity of the outflow channel. In the short-term then, lake surface elevations and volumes would exceed those predicted by the model, although values would approach model-predicted values as water is discharged downstream.

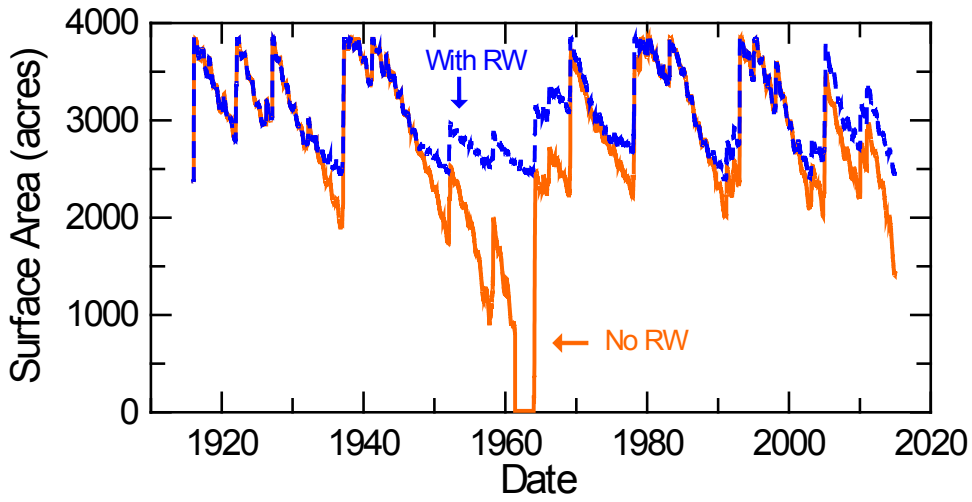

Fig. 2. Lake surface area with LEMP basin and natural flows (solid orange line) and supplemented inflows with recycled water (dashed blue line).

While it is difficult to discern from Fig. 3, outflows often occurred for several weeks or more, with the duration governed by the intensity and duration of runoff events (i.e., features in Fig 3 represent many days, rather than a single day). Also not necessarily evident, supplementation with recycled water increases the amount of water discharged to the outflow and Temescal Creek on similar dates, especially evident in late 1969 and 1979. For example, outflow occurred for an additional 53 days in winter 1969 with recycled water added, at a flow rate up to more than 5000 af/d and resulting in a cumulative additional outflow of 29,071 af (Fig. 4).

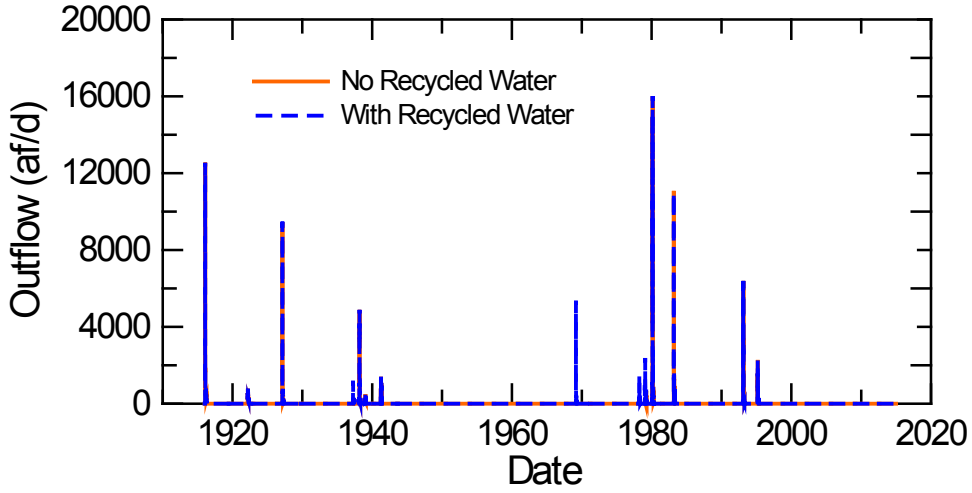

Fig. 3. Daily lake outflow from LEMP basin with natural flows (solid orange line) and inflows supplemented with recycled water (dashed blue line).

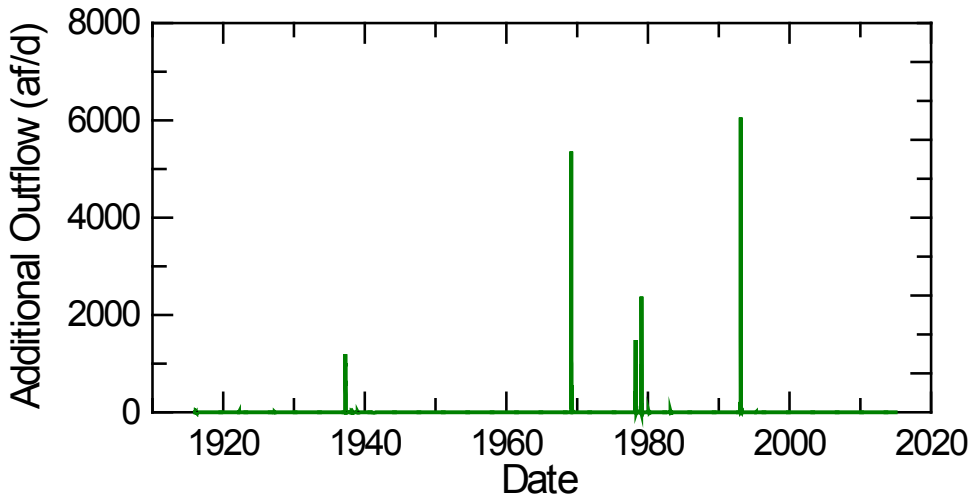

Fig. 4. Additional daily outflow from LEMP basin beyond that predicted for natural flows resulting from supplementation with recycled water.

Supplementation with recycled water also had a clear effect on total dissolved solids (TDS) concentrations in the lake (Fig. 5). Most notably, addition of recycled water eliminated the extreme TDS values (>10,000 mg/L) predicted for mid- to late-1950's through 1964 when lake surface elevation dropped to very low levels (Fig. 1) and eventually went dry (Fig. 2). Since supplementation with recycled water helps maintain water in the lake, TDS concentrations do not reach the extreme values present when the lake levels drops to exceedingly low values, thus providing a ceiling to TDS levels that is a function of TDS concentration in recycled water and the frequency and intensity of outflow-flushing events (Fig. 5).

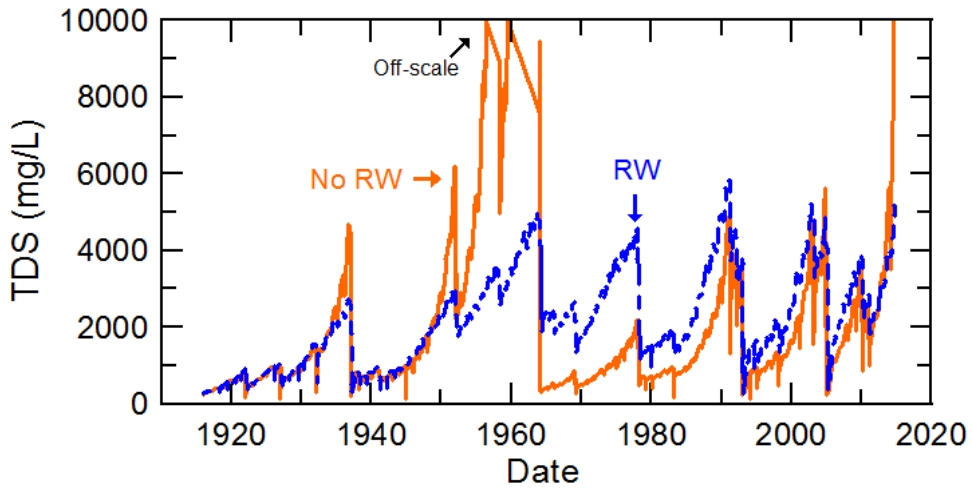

Fig. 5. TDS concentrations over time with LEMP basin and natural flows (solid orange line) and inflows supplemented with recycled water (dashed blue line).

The addition of recycled water also constrains the lower range of TDS predicted in the lake (Fig. 5). For the simulated interval since about 1960, recycled water supplementation yielded TDS levels that rarely dropped below 1,000 mg/L and were more typically predicted to be 2,000-4,000 mg/L (Fig. 5, blue line). Minimum TDS concentrations were much lower without recycled water additions (Fig. 5, orange line).

This can be seen from a cumulative distribution function for TDS with and without recycled water additions (Fig. 6). One notes that the exceedance probabilities differ significantly for the 2 scenarios, with lower TDS values predicted over 80% of the time for natural inflows relative to those with recycled water supplementation, although TDS values were dramatically higher without recycled water supplementation about 15% of the simulation period (Fig. 6). On no day was TDS predicted to exceed 6,000 mg/L with recycled water additions, while TDS values with only natural flows exceeded 6,000 mg/L 9.3% of the time (over 3300 days or >9 yrs out of 99). The median TDS value for the 99-yr simulation period under natural flows was 1,163 mg/L while the value increased to 2,055 mg/L with recycled water supplementation. Recycled water supplementation thus constrained TDS values to <6,000 mg/L, but also increased TDS levels much of the time. If we assume that TDS values >2,000 mg/L negatively impact the ecology of the lake, some salinity-impairments would be expected about 52% of the time with recycled water additions and 32% of the time with natural flows.

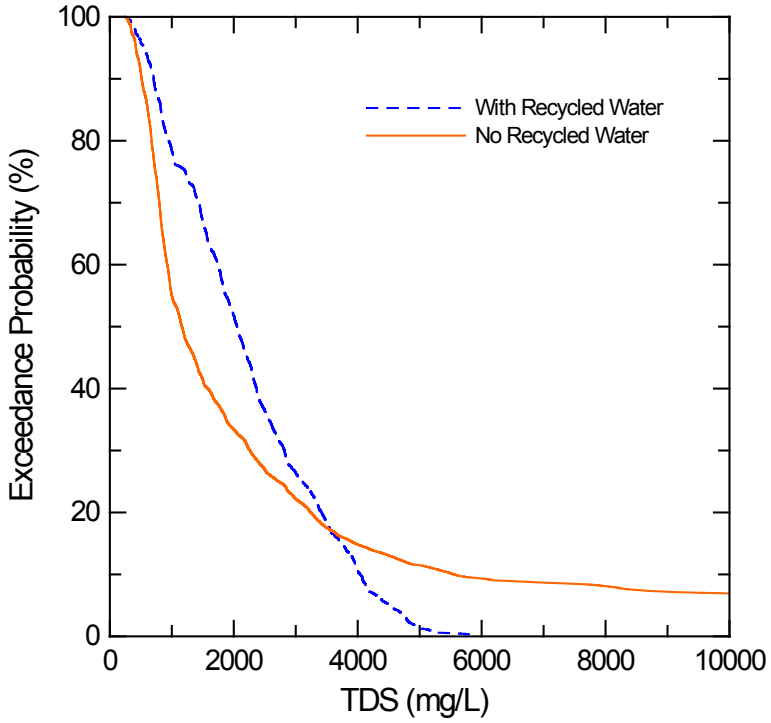

Fig. 6. Cumulative distribution function showing exceedance probability for TDS concentrations for the LEMP basin with natural flows (solid orange line) and inflows supplemented with recycled water (dashed blue line).

Of course, far less extreme conditions are predicted with recycled water (Fig. 6); most would probably agree that moderate lake levels (>1235 ft) (Fig. 1) and TDS values below 6,000 mg/L (Figs. 5 and 6) are preferable to very low lake levels, limited lake area, sea-water salinities or dry lake bed conditions predicted periodically with only natural inflows.

Importantly, the LEMP basin allows for periodic outflow and export of salt from the lake (Table 1). Natural flows delivered 1.55 MAF to the lake over the 1916-2014 simulation period, with 0.51 MAF (33%) flowing out in a limited number of years (Fig. 3). Supplementation with recycled water increased inflows to 1.77 MAF and outflows by 76,940 acre-feet to 0.58 MAF (Table 1). These outflows also exported salt; nearly 41% of the salt delivered to the basin with natural flows was removed with outflow, while a smaller fraction of a larger salt load, associated with recycled water inputs, was exported (35%) (Table 1). The 200,000 metric ton larger salt load to the lake with recycled water results from the higher salinity of that water relative to natural flows.

Table 1. Predicted total flows and salt budget for LEMP basin (99-yr simulation).

Scenario	Total Flow In (af)	Total Flow Out (af)	Total Salt In (tonnes)	Total Salt Out (tonnes)
No Recycled H_2O	1,546,230	506,982	535,972	219,245
+ Recycled H_2O	1,771,860	583,922	735,858	258,121

Conclusions

Simulations for Lake Elsinore using meteorological and runoff records from the past 99 yrs (1916-2014) with and without recycled water supplementation indicate:

(i) recycled water supplementation significantly increases lake surface elevation and lake area compared with natural inflows into the lake during periods of limited precipitation and runoff;

(ii) recycled water supplementation maintained predicted lake elevations >1234.5 ft and lake areas >2370 acres, while natural inflows resulted in complete desiccation of the lake for almost 3 yrs during the extreme drought that began in the late 1950s and continued into the early 1960s;

(iii) recycled water supplementation prevented extreme TDS levels from developing in the lake (keeping TDS concentrations <6000 mg/L) but also increased average TDS concentrations by about 900 mg/L, from 1,163 mg/L to 2,055 mg/L over the 99-yr (1916-2014) simulation period;

Next Step

The next step will be to extend this comparison of natural inflows with recycled water supplementation beyond lake level and salinity, and assess impacts of recycled water on concentrations of nutrients, dissolved oxygen, chlorophyll and other properties.

References

Anderson, M.A. 2015. *Technical Memorandum Task 1.0: Surface Elevation and Salinity in Lake Elsinore: 1916-2014.* Draft Technical Memorandum to LESJWA. 13 pp.

Anderson, M.A. 2013. *Predicted Effects of Lake Elsinore Management Project (LEMP) on Lake Level and Water Quality of Lake Elsinore.*

Technical Memorandum

Task 1.2: Water Quality in Lake Elsinore Under Pre-Development and Modern Land Use Conditions: Model Predictions for 1916-2014 with Current (post-LEMP) Basin

Objective

The objective of this task was to simulate water quality in Lake Elsinore using the current (post-LEMP) basin for the entire 1916-2014 period, comparing predicted water quality in the lake under pre-development and modern land use conditions. For this assessment, the current (post-LEMP) basin will be used for the entire simulation period.

Approach

The Computational Aquatic Ecosystem Dynamics Model (CAEDYM v.3) was linked to the 1-D Dynamic Reservoir Simulation Model (DYRESM v.4) model used in Tech Memos 1.0 and 1.1 that simulated lake level and salinity in Lake Elsinore for the period 1916-2014 (Anderson, 2015a,b). The CAEDYM model is a highly advanced ecosystem model capable of simulating a vast array of water quality and ecological parameters. In addition to the daily average meteorological conditions and runoff-streamflow volumes required by DYRESM, the structure of the food web, dynamics within the food web, rates of reactions for photosynthesis, nutrient uptake, excretion, mineralization, transformation, as well as nutrient concentrations in runoff and streamflow and a large number of other parameters and variables. The reader is referred to the CAEDYM Science Manual v.3.2 for additional details (Hipsey et al., 2014). For these simulations, 3 algal groups (blue-green algae, green algae and freshwater diatoms), 2 zooplankton groups (copepods and cladocerans), and 2 fish groups (approximately threadfin shad and larger piscivores such as bass and crappie) will be represented. Consistent with the TMDL developed for Lake Elsinore, we will focus on 4 key water quality parameters: total N, total P, dissolved oxygen (DO) and total chlorophyll a.

Model Calibration: 2000-2014

Key Input Parameters

The coupled DYRESM-CAEDYM model was calibrated against available data for 2000-2014. Meteorological conditions that drive the hydrodynamics in the 1-D DYRESM model were taken from the CIMIS station #44 at UCR (Fig. 1). Key forcing factors driving the heating, cooling and mixing of Lake Elsinore include the shortwave solar heat flux (300-3000 nm) that includes photosynthetically available radiation (PAR, 400-700 nm), as well as near-UV (300-400 nm) and near-IR and IR (700-3000 nm) (Fig. 1a), air temperature (Fig. 1b) and windspeed (Fig. 1c). Values are represented as daily average values. The strong seasonal trend in solar shortwave heat flux is evident in the figure,

with daily average shortwave flux values of about 350 W/m2 in the summer and 50-100 W/m2 during the winter (Fig. 1a). Daily average air temperatures exhibit a similar seasonal pattern, with daily-averaged summer temperatures near 30°C and daily average winter temperatures generally 7-10°C (Fig. 1b). Daily average windspeeds averaged near 2 m/s and exhibited some seasonality as did daily rainfall rates that also showed annual variability (Fig. 1c,d).

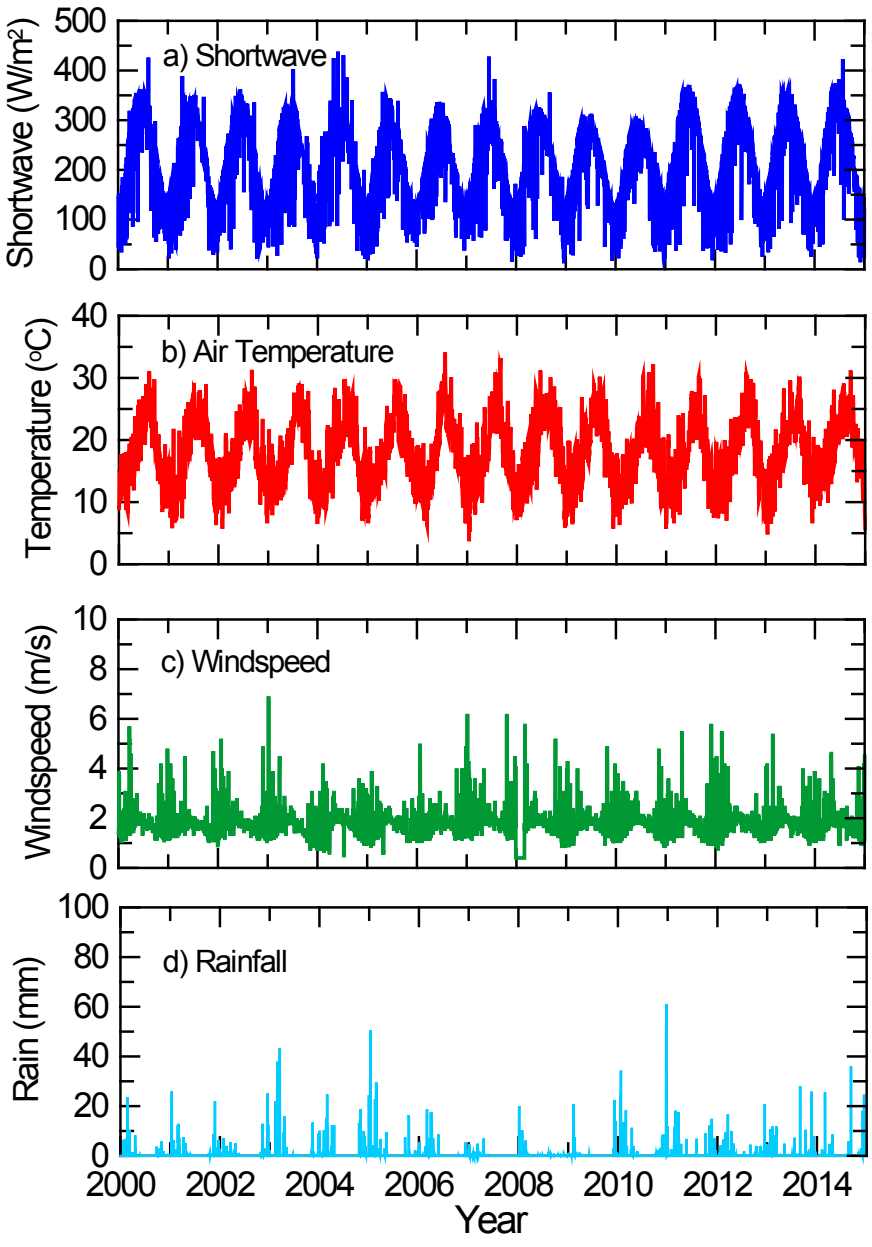

Fig. 1.

In addition to direct precipitation on the lake surface, water delivered to the lake included San Jacinto River flows (as recorded at the USGS gage #11070500), runoff

from the local watershed (Anderson, 2015a), and supplemental water that included recycled water from EVMWD as well as recycled water from EMWD and water pumped from island wells in 2003-2004 (collectively represented as recycled water) (Fig. 2).

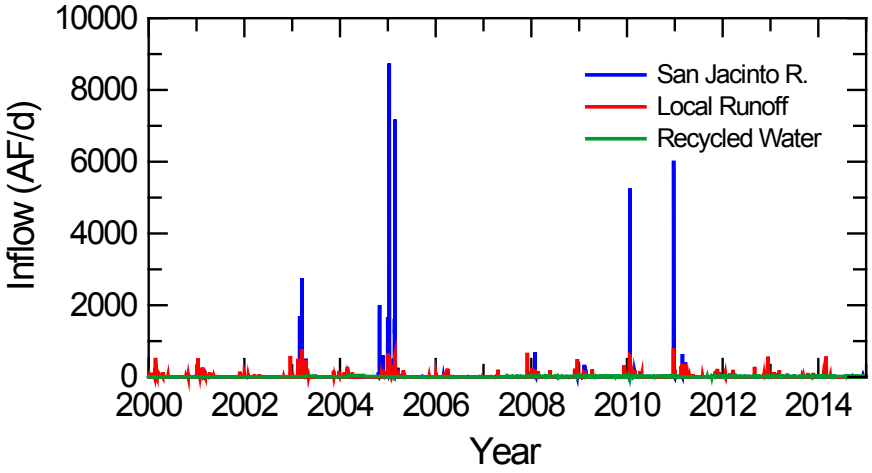

Fig. 2.

External loading of nutrients was derived from inflows from the San Jacinto River, local runoff and recycled water (Fig. 2). A limited number of large runoff events delivered most of the flows from the San Jacinto River during this time period, including the very large runoff events at the beginning of 2005, that included daily flow exceeding 8,000 acre-feet (Fig. 2, blue line). Shorter duration high flow runoff events were also present in January 2010 and December 2011. Precipitation generated runoff from the local watershed as well, although daily flows were much smaller than the very large runoff events noted in 2005, 2010 and 2011 (Fig. 2). Recycled water flows were much lower than runoff volumes and barely perceptible on Fig. 2 (green line). Presented as cumulative flows however, we see that recycled water inputs exceeded that of local runoff and contributed about 50,000 acre-feet since inputs began in late 2002 (Fig. 3). Based upon these values, a total of 187,926 acre-feet of water was delivered to Lake Elsinore over this 2000-2014 period, with approximately 53% derived from San Jacinto River flows, 20% from local runoff and 27% from recycled water (Fig. 3a).

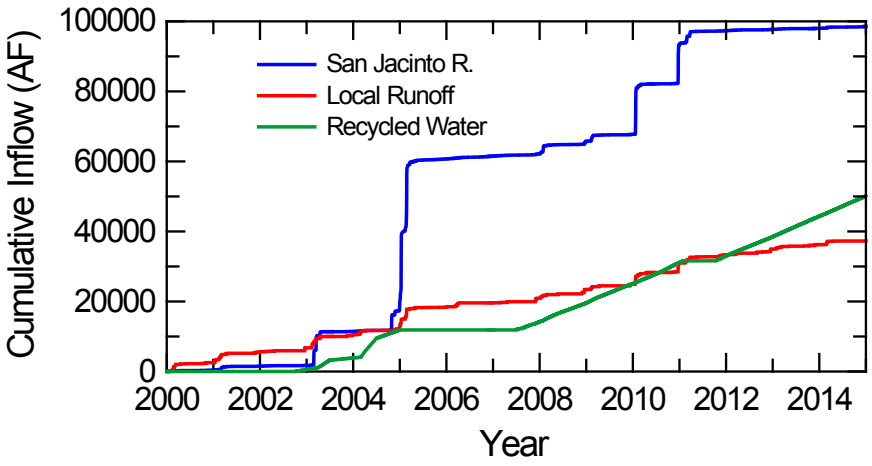

Fig. 3.

Concentrations of nutrients in these inflows vary depending upon a number of factors, including intensity and duration of storms, interval of time between storms and other factors (including treatment plant operation for recycled water inputs). Average concentration values derived from runoff sampling within the watershed and treatment plant data were used in model simulations (Table 1).

Table 1

Source	PO_4-P	Total P	NH_4-N	NO_3-N	Total N
San Jacinto R.	0.28	0.50	0.22	0.57	1.62
Local Runoff	0.20	0.48	0.22	0.80	1.82
Recycled H2O[a]	0.32	0.41	0.36	1.62	2.87

[a]*Recycled water concentrations for EVMWD 2007-present.Higher concentrations of PO_4-P, NH_4-N and NO_3-N were present for the 2002-2004 period which included significant volumes of island well and EMWD flows (concentrations for this period of 0.82, 0.24 and 10 mg/L, respectively).*

Total external nutrient loading over the calibration period was calculated from flow data (Fig. 2) and nutrient concentrations (Table 1). Flows from the San Jacinto River comprised delivered 47% of the total external load of PO_4-P (71,848 kg) added between 2000-2014, with 40% from recycled water supplementation, and 13% from local watershed runoff (Fig. 3). Recycled water contributed 63% of the total TIN load, while San Jacinto River and local runoff contributed 25 and 12%, respectively. From Fig. 3, we note that the contributions of PO_4-P from the 3 sources are broadly comparable to their volumetric flow contributions owing to broadly similar PO4-P concentrations (Table 1), while recycled water contributes a disproportionately large amount of TIN based upon it total flow owing to its larger NO_3-N concentration.

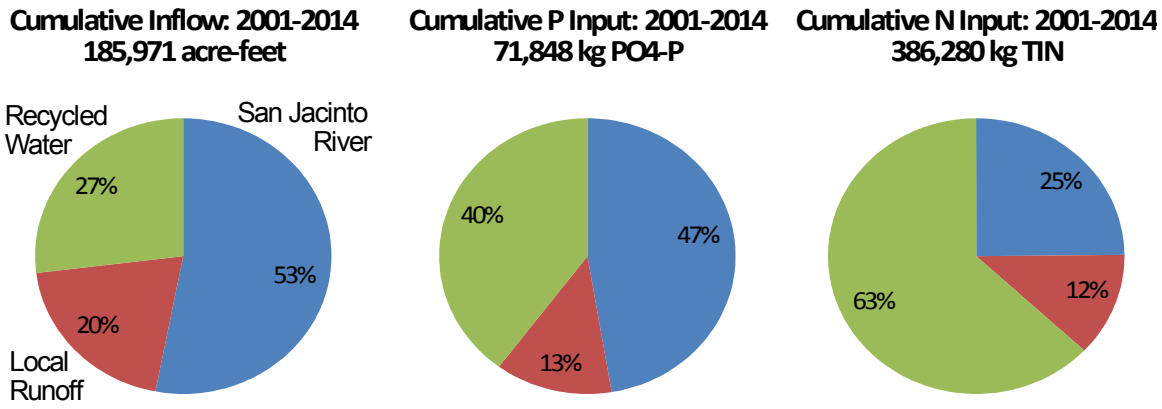

Fig. 3.

Temperature

The model reasonably captured measured temperature values in Lake Elsinore (Fig. 4). The model correctly predicted strong seasonal trends in water column temperature that reflects seasonal trends in solar shortwave heat flux (Fig. 1a) and air temperature (Fig. 1b). The model predicted summer values near 27°C and winter minimum values near 10°C, with little difference between depths reflecting weak stratification or mixed conditions commonly present in the lake (Fig. 4).

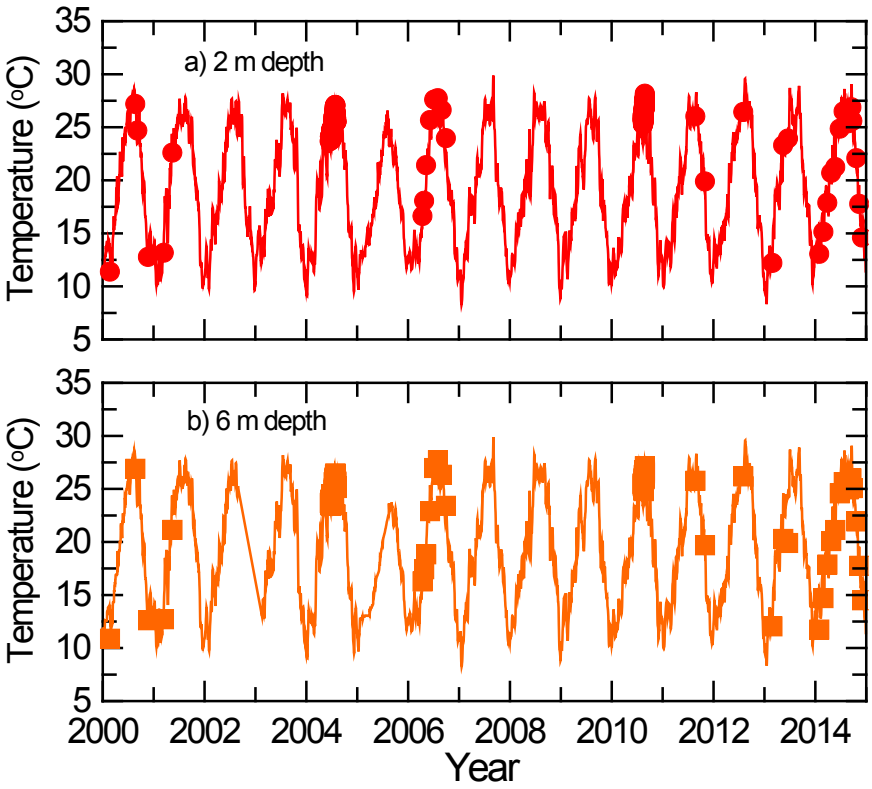

Fig. 4.

Dissolved oxygen (DO) in the lake varied seasonally and with depth (Fig. 5). The temperature effect on oxygen solubility was evident in model predictions for the 2 m depth, with DO values generally near 10 mg/L in the winter and 7-8 mg/L in the summer (Fig. 5a). At the same time, supersaturation was periodically predicted (e.g, in spring 2011 when concentrations reached 17 mg/L). The model predicted DO concentrations deeper in the water column to be often quite similar to near-surface values, but did also correctly predict periods of anoxia in the summer of 2003, 2004, 2006 and 2010 (Fig. 5b).

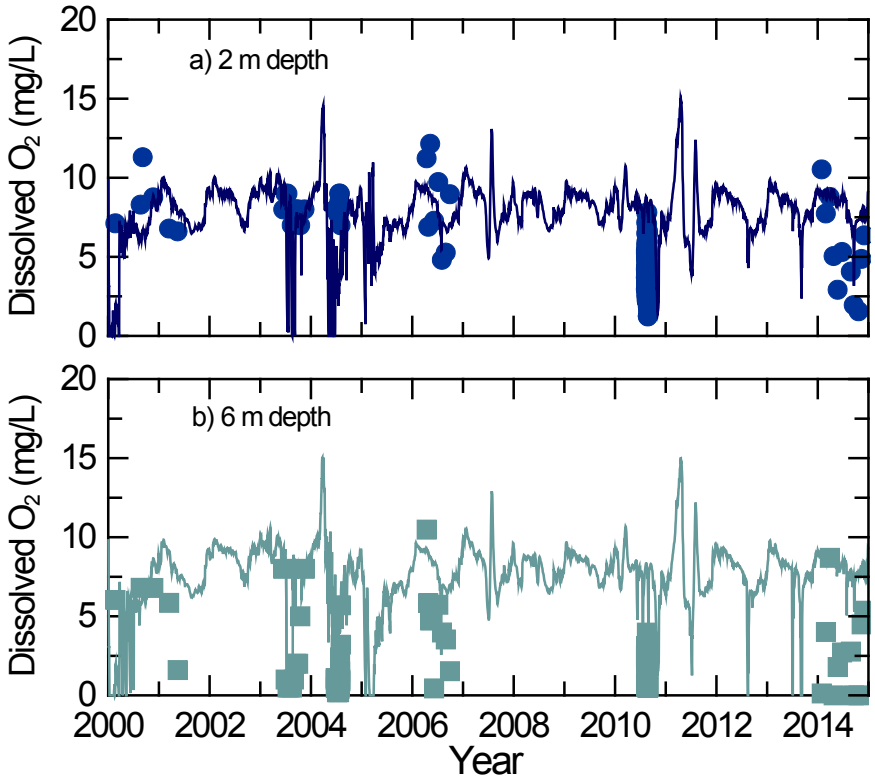

Fig. 5.

The model did a fair job of capturing the dramatic trends in concentrations of total N in the lake between 2000 and 2020 (Fig. 6). Concentrations increased from about 2 mg/L in 2000 to greater than 8 mg/L by late 2004, and then declined sharply with the very large runoff volumes delivered in winter of 2005 that quadrupled the volume of the lake. Total N concentrations then edged up over several years before declining slightly in 2010 (Fig. 6). While the model captured trends reasonably well, it did not reproduce the more significant apparent swings observed, e.g., in 2008, when reported concentrations over the period of a few months ranged from <1 to >8 mg/L. It may be that sampling bias or analytical challenges crept into the time series data, exaggerating short term trends.

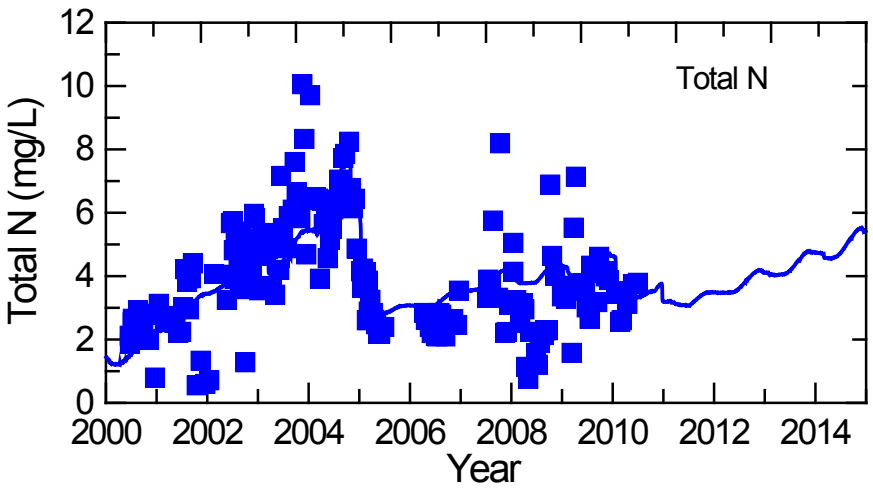

Fig. 6

Total P concentrations also varied quite dramatically over this calibration period, from about 0.1 mg/L in 2000 to >0.6 mg/L in late 2004 before declining to a value near 0.2 mg/L (Fig. 7). The model generally captured trends but underpredicted concentrations somewhat in 2003-2004, although it did predict a maximum value of about 0.6 mg/L in late 2004 (Fig. 7).

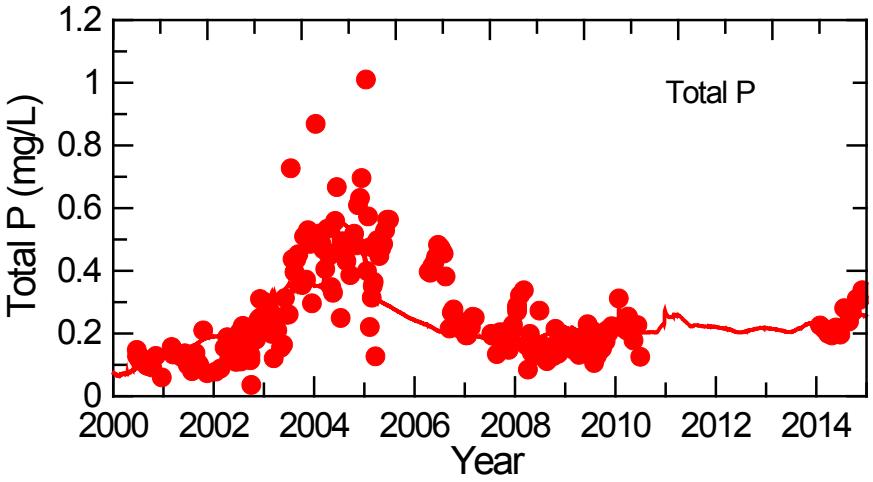

Fig. 7

Measured chlorophyll a concentrations exhibited pronounced seasonal and interannual variability, ranging from <10 µg/L in some winters to >300 µg/L in 2002, 2004 and 2014 (Fig. 8, solid symbols). The model did a fair job overall in reproducing these complex trends and corrected predicted summer maximum chlorophyll a concentrations in 2000-2004 (Fig. 8, line). The model did not do as well predicting the winter minimum values however, and also missed the particularly high concentrations observed in 2014 (Fig. 8). Notwithstanding, the agreement between predicted and observed

concentrations was considered passable given the highly dynamic algal dynamics in the lake and the complex dependence of chlorophyll a concentrations on nutrient availability and ecosystem structure.

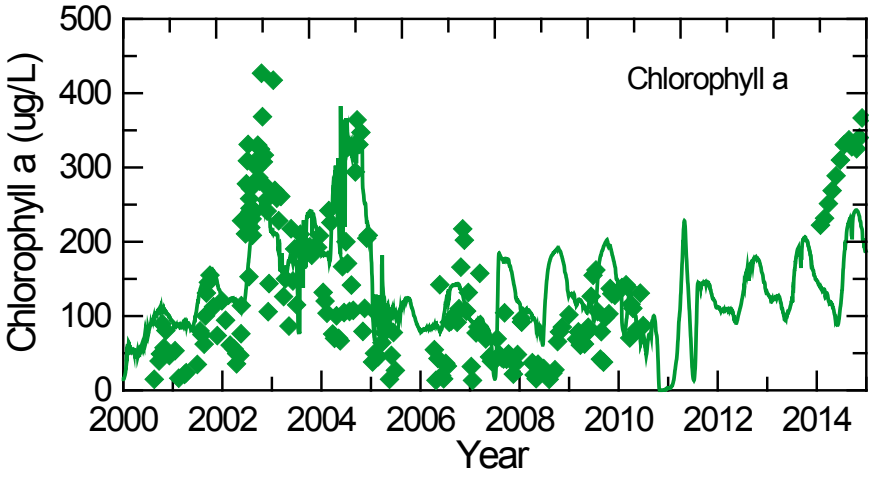

Fig. 8

The overall goodness of fit of the model results to measured concentrations of total N, total P and chlorophyll a was assessed using the relative percent error (RPE) between predicted and observed average concentrations (Table 2). Total N averaged 3.98 mg/L over this period, while the model yielded an average value of 3.88 mg/L, representing a 2.5% underestimate (Table 2). The average observed total P concentration over this period was 0.265 mg/L while the predicted average concentration was 0.235 mg/L, an 11.3% underestimate. Predicted and observed chlorophyll a concentrations wer 130 and 137 µg/L, corresponding to an RPE of 5.4%. Given the extreme range in conditions experienced at the lake over this 2000-2014 period, the model was considered to reasonably predict water quality in Lake Elsinore under a wide range of hydrologic, chemical and ecological conditions.

Table 2.

	Observed	**Predicted**	**% Error**
Total N	3.98	3.88	-2.5
Total P	0.265	0.235	-11.3
Chlorophyll a	130	137	+5.4

Technical Memorandum

Task 2.1: Stable Isotope, Elemental and Mobile-P Measurements in Lake Elsinore Sediments*

Objective

The objectives of this task were to quantify properties of Lake Elsinore sediments over time and correlate observed properties with hydrologic conditions, management actions and other factors.

Approach

Sample Collection

Two replicate cores were collected from profundal sediment ("Site 6", 33.66879° N, 117.35127° W) in Lake Elsinore on July 17, 2014 with a 1 meter polycarbonate tube with a 6.5 cm diameter. Water was carefully siphoned off the top of each core and the sediment was sectioned into 1 cm (for the top 10 cm) or 2 cm (for sediment deeper than 10 cm) intervals. Each section was homogenized and stored at 4°C under N_2 (g) in 50 mL polypropylene centrifuge tubes. A subsample from each interval was used for water content determination. To calculate water content, the wet sediment was pre-weighed into small aluminum pans and oven-dried at 105°C until reaching a constant weight (1-2 days).

Water was collected from 0.5 m depth at Site 6 on September 17, 2014 and June 18, 2015 and analyzed for isotopic composition of suspended organic matter (mainly phytoplankton). The water was stored in 20 L Nalgene jugs at 4°C until later filtration. The water collected in 2014 was stored for six months, over which it experienced an unknown period of time at 25°C, due to technical issues. Therefore suspended organic matter (SOM) experienced some decay over this period of time, but is thought to reflect, to at least some degree, natural decomposition processes operating within the lake.

Elemental Composition (XRF)

Bulk elemental composition was determined on sediment samples using a Spectro XEPOS HE Benchtop X-ray Fluorescence Spectrometer flushed with 85 L hr^{-1} of helium gas (EPA Method 6200). Approximately 5 g of wet sediment from sediment core interval was dried at 50°C and ground with a mortar and pestle prior to X-ray fluorescence analysis. Four different source energies/excitation targets were utilized per sample at count times of 200 seconds: excitation energy of 40 kiloelectron volts (kV) and 1 mA current; 60 kV and 0.66 mA; 25 kV and 1.6 mA; 20 kV and 2 mA.

**This technical memorandum was developed from Chapter 2 of the M.S. thesis of Simone Boudreau (2015).*

Phosphorus Forms

Forms of P in bottom sediment were extracted using the fractionation scheme described in Pilgrim et al. (2007). 0.2-0.25 grams of wet sediment was added to 50 mL polycarbonate centrifuge tubes, followed by a sequential phosphate extraction which utilized different reagents to measure the amount of phosphate in three different fractions within the sediment. The reagent solutions were 1M ammonium chloride (NH_4Cl) which extracts pore-water and loosely-sorbed P, followed by bicarbonate buffered dithionite solution (0.11M $NaHCO_3$/0.11M NaS_2O_4) to extract redox-sensitive P bound to iron and manganese hydroxides (Fe-P), and lastly 0.1M sodium hydroxide, NaOH, to extract non-reducible, aluminum-bound P (Al-P). The sum of the phosphate extracted in the first two steps represents mobile phosphorus, or phosphorus that can be re-released to the water column under low DO conditions. Aluminum-bound phosphate is generally considered to be a recalcitrant form that will not be re-released. 10 mL of each extract was added to the centrifuge tube. After each sequential reagent addition, the samples were placed on a shaker table for varying amounts of time: two hours for loosely-sorbed P, one hour for Fe-P, and 16 hours for Al-P (Pilgrim et al., 2007). Subsequent to each reagent addition and mixing, samples were centrifuged at 3,000 rpm for 20 minutes. The supernatant was decanted, filtered through 0.45 µm membrane filters, and stored in 20 mL HDPE scintillation vials in the freezer until analysis. The residual sediment continued on in the procedure after the supernatant from each step was decanted. One out of every 10 samples was replicated and 2 method blanks per core were used (no sediment, just reagent and centrifugation). Soluble reactive phosphorus was determined colorimetrically for each supernatant on a Seal AQ2 discrete analyzer following the automated ascorbic acid reduction method 4500-P F (Standard Methods for the Examination of Water and Wastewater, 20th edition). Absorbance was measured at 880 nm. Calibration control blank and calibration control verifications were used to verify accuracy.

Stable Isotopic Composition

Sediment subsamples were dried at 50°C and ground to a homogenous mixture with a mortar and pestle. The dried sediment was fumigated with concentrated HCl (12N) in a desiccator for 24 hours in order to remove inorganic C. Replicate samples were analyzed without fumigation to ensure all $CaCO_3$ had been removed. Suspended organic matter from epilimnetic water was filtered through 47 mm Whatman glass microfiber filters and then oven-dried at 50°C. Stable C and N isotope compositions as well as %OC (weight percent) and %N were analyzed on a Costech elemental analyzer coupled to a Delta V Advantage Isotope Ratio Mass Spectrometer at the Facility for Isotope Ratio Mass Spectrometry (FIRMS) at University of California, Riverside. One in every ten samples was replicated.

Results

Using the sedimentation rate of 1.27 cm/year previously determined by Byrne et al. (2004), the dates corresponding to given sediment depths were calculated using the formula shown below and plotted on each depth profile as a secondary y-axis to allow comparison of sediment properties over time and with lake management activities.

$$t = t_0 - (z/1.27 \text{ cm yr}^{-1}) \quad (1)$$

where t = date (decimal year) at sediment depth z

t_0 = date at time of sediment collection (2014.5)

z = sediment depth (cm)

Historical lake management activities are summarized in Fig. 1 for reference. Prior to the completion of the Lake Elsinore Management Project (LEMP) in 1995, Lake Elsinore was larger and shallower with presumably greater mixing and circulation. The completion of the project in 1995 marks the transition to a deeper lake with a reduced surface area. Addition of supplemental recycled wastewater began in 2002 and continued through 2004 and from 2008-present. Lake level varied strong over this period due to periodic drought and El Nino events.

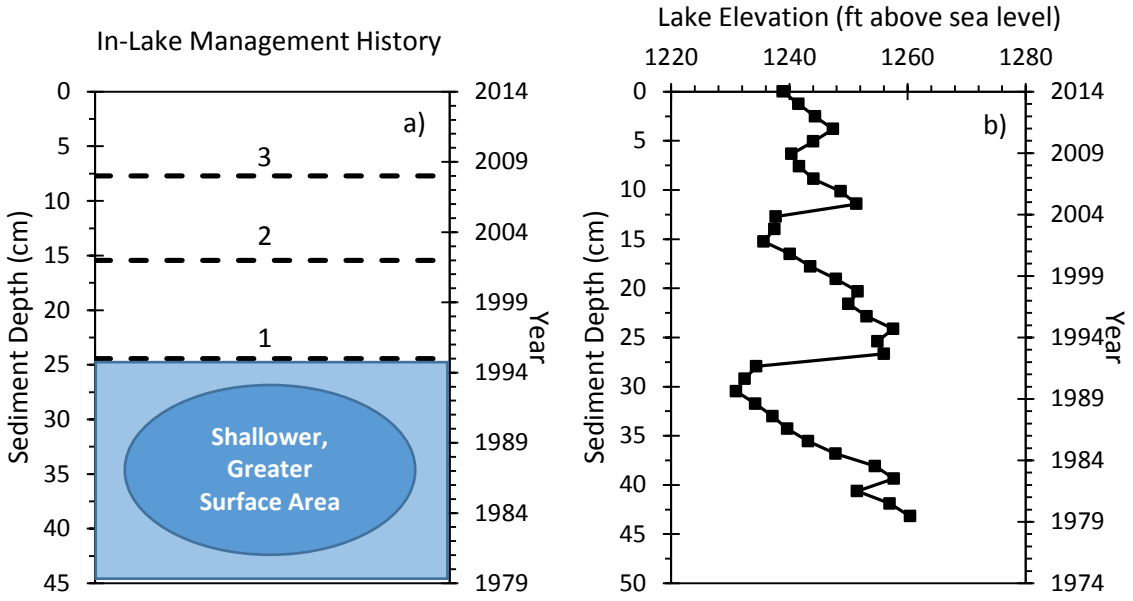

Fig. 1. Lake Elsinore: a). historical lake management: 1=Completion of LEMP, 1995. 2=Supplemental recycled wastewater begins, 2002. 3=Aeration system begins operating, 2008; b) lake surface elevation in feet above sea level.

Water Content

Water content of sediment increased with decreasing depth (and time), from about 70% to 90%, with the exception of a decrease in water content (which is reflected in both replicates) from depth of 22 cm to 10-16 cm in cores 6-A and 6-B (Fig. 2).

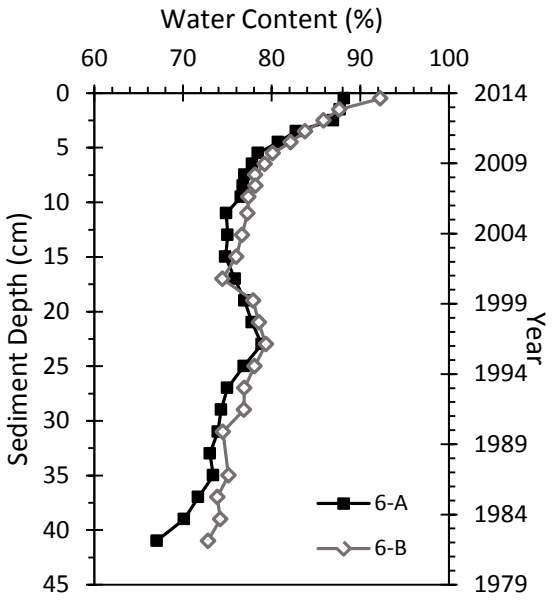

Fig. 2. Water content (%) with sediment depth at Site 6.

Elemental Composition

Organic carbon increases by 5% (from approximately 2% to 7%) from the bottom to the top of the cores (representing freshly deposited sediment). Organic carbon and total nitrogen concentrations reflect an increase from 30 cm to 25 cm as well as an increase up-core in the top 10 cm. Nitrogen increases from 0.25 to 0.75% throughout the length of the cores. Organic carbon and nitrogen are significantly correlated in both cores (r=0.97) (Table 1). The gradual increase in OC in the top 10 cm reflects an exponential increasing trend with decreasing depth, as the data better fit an exponential function (average r^2=0.77) than a linear function (average r^2=0.70). Similarly, the up-core increase in N in the top 10 cm better fits an exponential function (r^2=0.70) than a linear function (r^2=0.62). OC:N remains relatively constant with depth in both cores, at a value of 10, with minor fluctuations. OC:N of suspended organic matter collected in June 2015 was 6.9±0.2. Total phosphorus increases from 0.1% at the bottom of the core to 0.15% at the top of the core. TP exhibits an up-core exponential increase in the top 10 cm (r^2 =0.74 vs r^2 =0.71 for linear fit). The depth profiles for silicon and aluminum reveal an increase between 25 and 30 cm after which the concentrations return to background levels and remain relatively constant to the top of the cores. Silicon and aluminum are significantly correlated (r =0.99), and their stoichiometric ratios suggest the presence of alumino-silicate minerals such as montmorillonite (Wetzel, 2001) which has a 2:1 molar ratio of Si to Al. Calculation of the ratio of moles of Si per gram (0.006) to moles Al per gram (0.003) in Lake Elsinore sediments resulted in a value of 2. Sulfur (S) increases from 6000 µg/g in 1989 to 2000 µg/g in 1994 after which it remains constant

with sediment depth. Calcium (Ca) increases from 4% at the bottom of the core to 10% at the top. The increase is not a gradual, constant increase. Instead calcium increases from the bottom of the core to 25 cm (1994). It remains constant from 1994 to 10 cm (2007), after which it increases exponentially to the top of the core (r^2 = 0.86 for exponential fit, vs. r^2 =0.83 for linear fit).

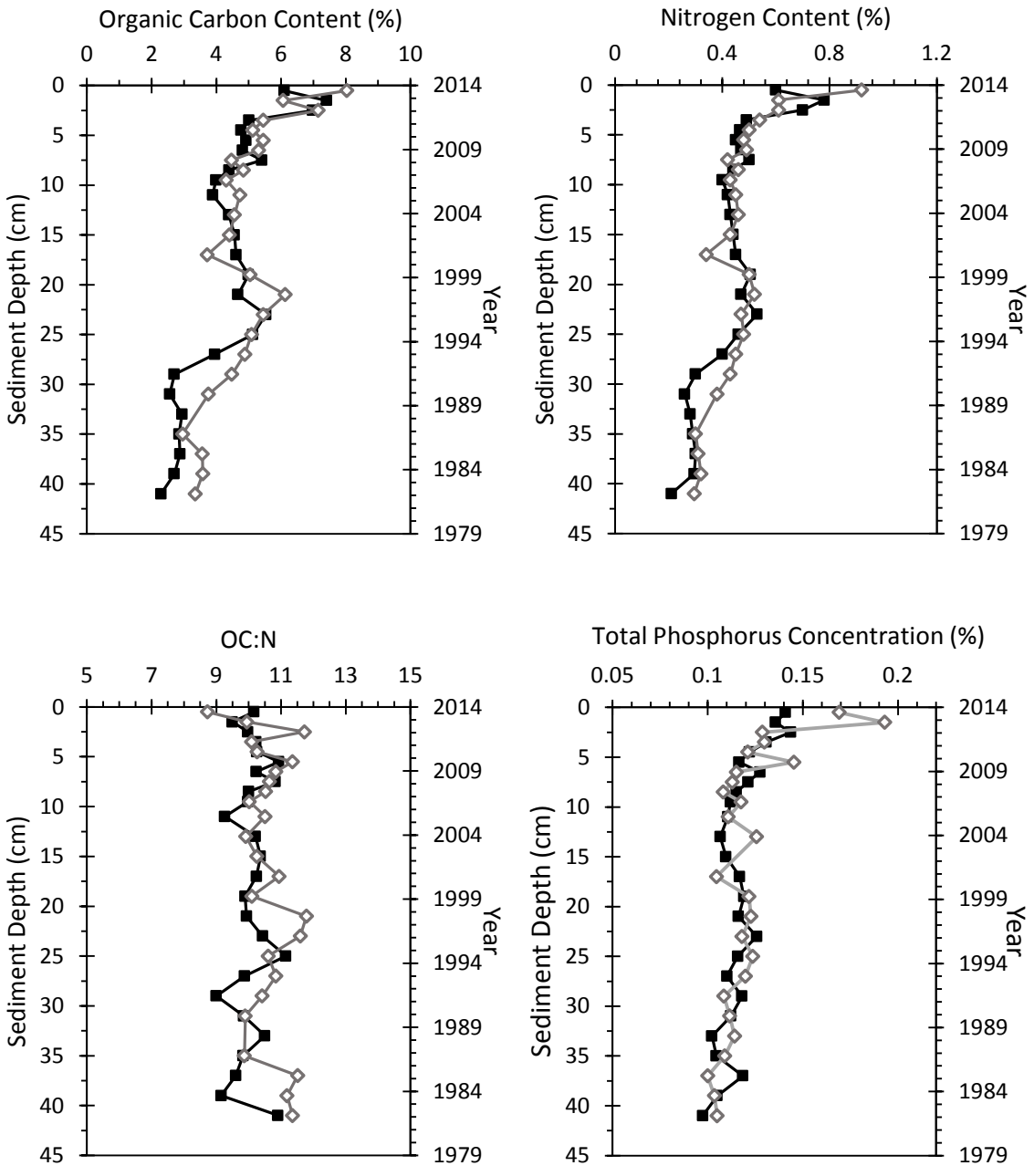

Fig. 3. Organic carbon content, total nitrogen content, OC:N ratio, and total phosphorus concentration in Lake Elsinore sediment. Solid squares represent data points in core 6-A. Open diamonds represent data points in core 6-B.

Calcium also exhibits a significant correlation with OC and N (Table 1). Iron shows a similar but opposite trend as calcium, decreasing until 1994, remaining relatively constant until 2006, then decreasing to the top of the core. The overall decline in concentration is 6.25 to 5%. Iron and calcium are significantly negatively correlated (Table 1).

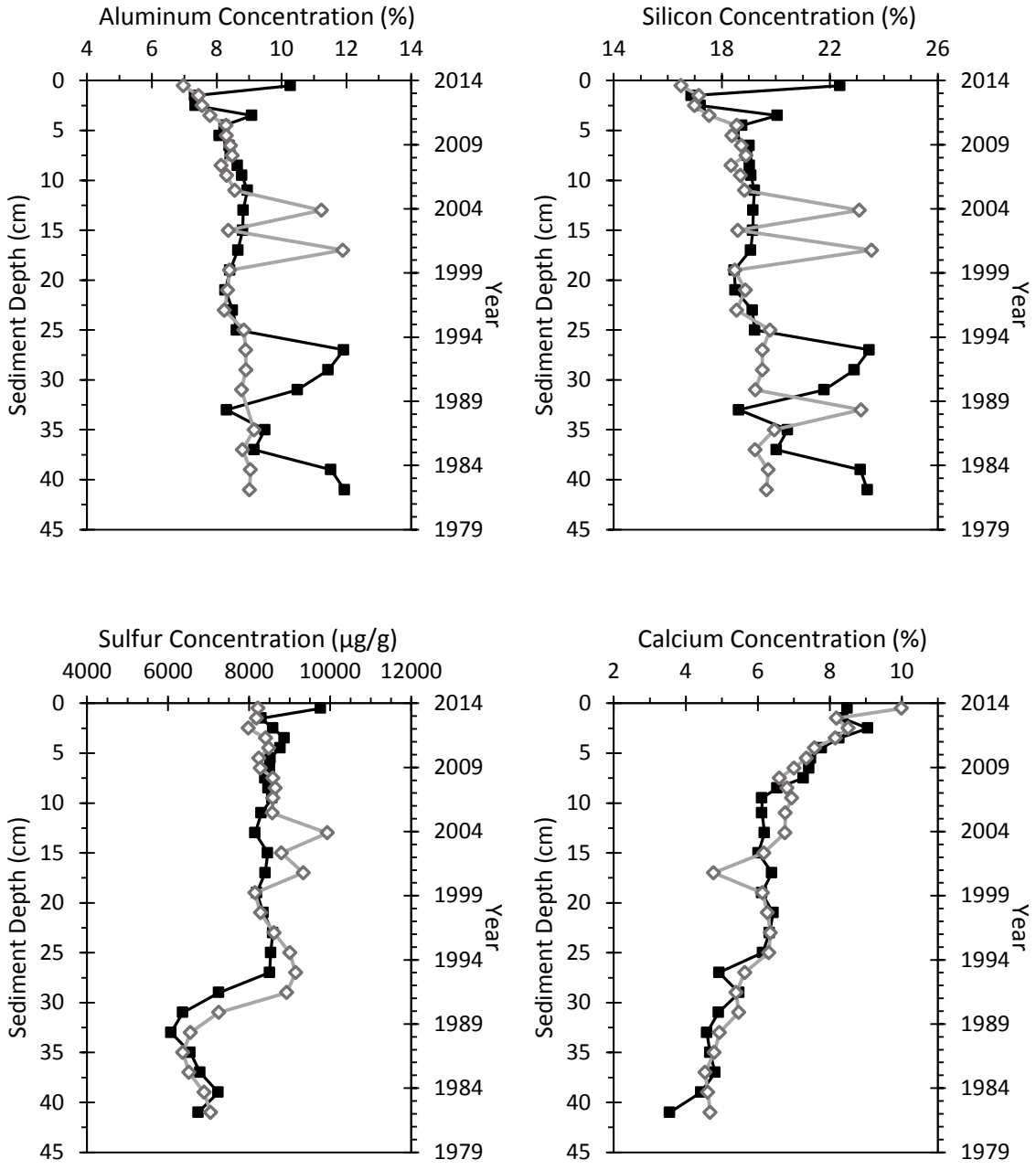

Fig. 4. Aluminum, silicon, sulfur, and calcium depth profiles of Lake Elsinore sediment. Solid squares represent data points in core 6-A. Open diamonds represent data points in core 6-B.

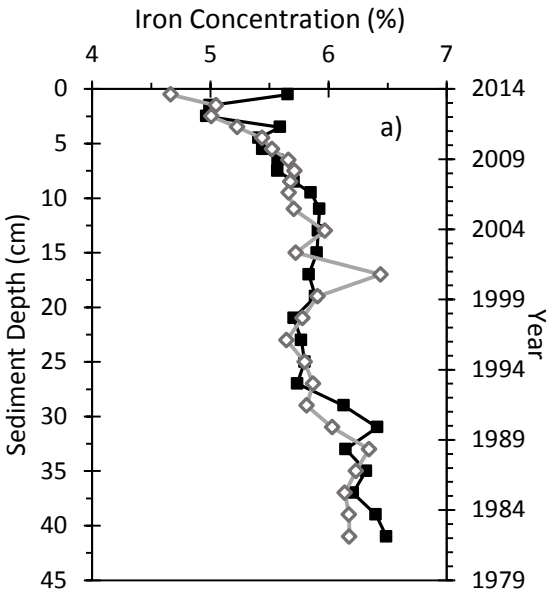

Fig. 5. Iron concentration profiles for Lake Elsinore sediment. Solid squares represent data points in core 6-A. Open diamonds represent data points in core 6-B.

Table 1. Correlation table showing r values for bulk elemental properties in Lake Elsinore sediment. With n=26, an r value of 0.51 is statistically significant at p=0.001.

	Depth	Water	%OC	%N	Al	Si	P	S	K	Ca	Ti	Fe
Depth	1.00											
Water	-0.79	1.00										
%OC	-0.75	0.89	1.00									
%N	-0.75	0.91	0.97	1.00								
Al	0.48	-0.56	-0.62	-0.59	1.00							
Si	0.48	-0.53	-0.60	-0.57	0.99	1.00						
P	-0.57	0.72	0.63	0.68	-0.39	-0.35	1.00					
S	-0.67	0.49	0.58	0.57	-0.04	-0.02	0.43	1.00				
K	0.91	-0.79	-0.86	-0.85	0.58	0.58	-0.58	-0.73	1.00			
Ca	-0.90	0.94	0.88	0.90	-0.60	-0.58	0.70	0.56	-0.88	1.00		
Ti	0.88	-0.87	-0.87	-0.87	0.50	0.50	-0.65	-0.66	0.95	-0.93	1.00	
Fe	0.81	-0.89	-0.89	-0.90	0.70	0.69	-0.66	-0.49	0.91	-0.93	0.94	1.00

Phosphorus Forms

Redox-sensitive phosphate is the least abundant fraction, averaging about 75 µg/g dry weight (dw) throughout the length of the cores and remaining constant with depth (Fig. 6, open diamonds). Loosely-sorbed and pore-water phosphate represents the majority of the mobile-P (~60%) (Fig. 6, solid triangles). With the exception of two noticeable increases at 20 and 35 cm, loosely-sorbed/pore-water P remains at about 150 µg/g dw below 10 cm depth. In the upper 10 cm, the fluctuations stabilize, and smaller variations center around 125 µg/g dry weight. This signifies a shift to lower pore-water P concentrations in more recently deposited sediment. Aluminum-bound P was the most abundant of the fractions measured using the sequential extraction procedure, with concentrations ~135 µg/g dw at the bottom of the core (Fig. 6, solid squares). The concentration exhibits a large increase to ~200 µg/g dw at about 25 cm, followed by a shift to greater concentrations in depths <25 cm, averaging 150-160 µg/g dw. The increase and subsequent shift to greater mean concentrations occurred in 1994, around the same time the Lake Elsinore Management Project was completed (Figs. 1, 6).

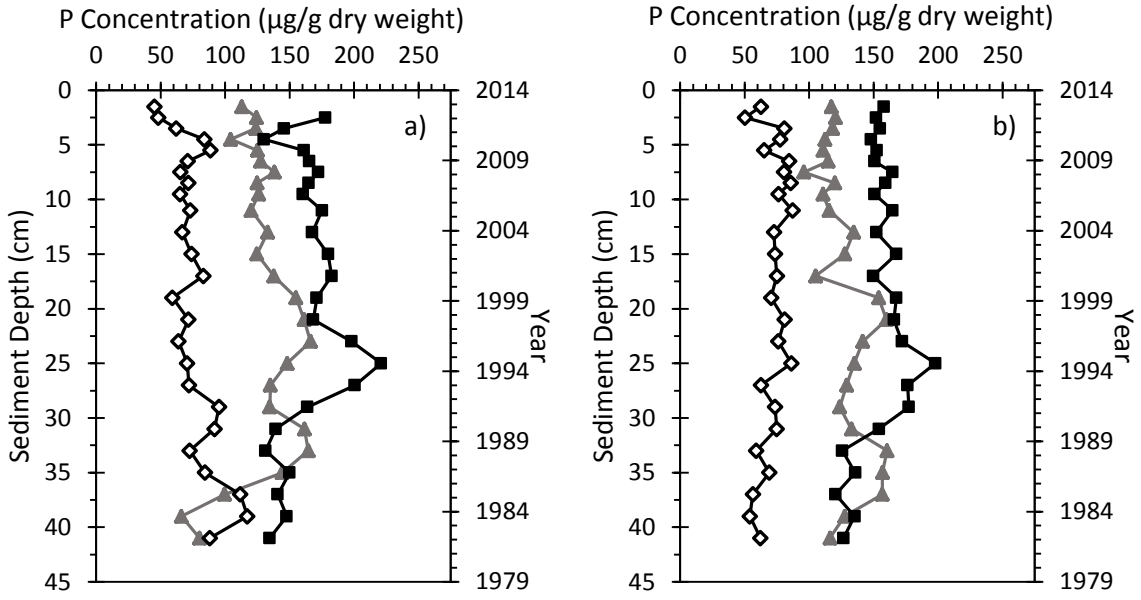

Fig. 6. Phosphorus concentrations in three different sediment forms. Panel a shows core 6-A. Panel b shows core 6-B. Open diamonds=Fe-P. Solid triangles= loosely-sorbed/pore-water P. Solid squares=Al-P. Mobile-P is taken as the sum of loosely-sorbed/pore-water P and Fe-P.

Stable Isotopic Composition

Stable isotopic composition results are presented in delta notation relative to Vienna Pee Dee Belemnite Standard (for C) and Air N_2 standard (for N) and calculated using the equation, exemplified below for ^{13}C:

$$\delta^{13}C = \left[\left(\frac{{}^{13}C/_{12}C_{sample}}{{}^{13}C/_{12}C_{standard}} \right) - 1 \right] * 1000 \quad (2)$$

The filters exhibited suspended organic matter (SOM) with $\delta^{13}C$ values of -20.2±0.6‰ and -23.7±0.4‰ in the fresh and decomposed samples, respectively (Table 2). The measured $\delta^{15}N$ of the SOM was 5.8±0.2‰ and 10.2±1.6‰ in the fresh and decomposed samples, respectively. The decomposed SOM exhibited about a 3‰ higher $\delta^{15}N$ than the top of the sediment core and about a 4‰ more negative $\delta^{13}C$ than the top sediment. Fresh SOM reflected the same $\delta^{13}C$ values as the top sediment and slightly lower (0.7‰ difference) $\delta^{15}N$.

$\delta^{13}C$ values are gradually increasing in both cores from approximately -24‰ at 29 cm to -20‰ at the top of the cores (Fig. 7). In core 6-A, $\delta^{13}C$ increases from -25‰ at the bottom of the core to -20‰ at the top of the core. This gradual 5‰ increase towards the top of the core represents a significant change with depth (r^2=0.72).

The $\delta^{15}N$ depth profiles reflect three distinct periods which have significantly different mean values. From 41 to 35 cm (the bottom section of the core), mean $\delta^{15}N$ values are 6.2±0.4‰ and 6.5±0.4‰ for cores 6-A and 6-B, respectively. This section represents the time frame from approximately 1982 to 1988, when the lake was shallow, prior to completion of the Lake Elsinore Management Project. After 1988, during the transition from a shallower, larger surface area lake to a deeper lake with a smaller surface area, $\delta^{15}N$ shifts to lower, more variable values with means 5.3±0.5‰ and 5.8±0.4‰. This period lasts from 31 cm to 17 cm (1990-2001), after which point the signatures increase to 7.1±0.4‰ and 6.9±0.6‰ in cores 6-A and 6-B, respectively. In the top layer of sediment, $\delta^{15}N$ values vary little and the high values extend to the top of the cores.

Table 2. Stable isotopic composition of suspended organic matter (SOM)

Suspended Organic Matter	$\delta^{13}C$ (‰ vs. VPDB)	$\delta^{15}N$ (‰ vs. Air N_2)
Fresh	-20.2±0.6	5.8±0.2
Decayed	-23.7±0.4	10.2±1.6

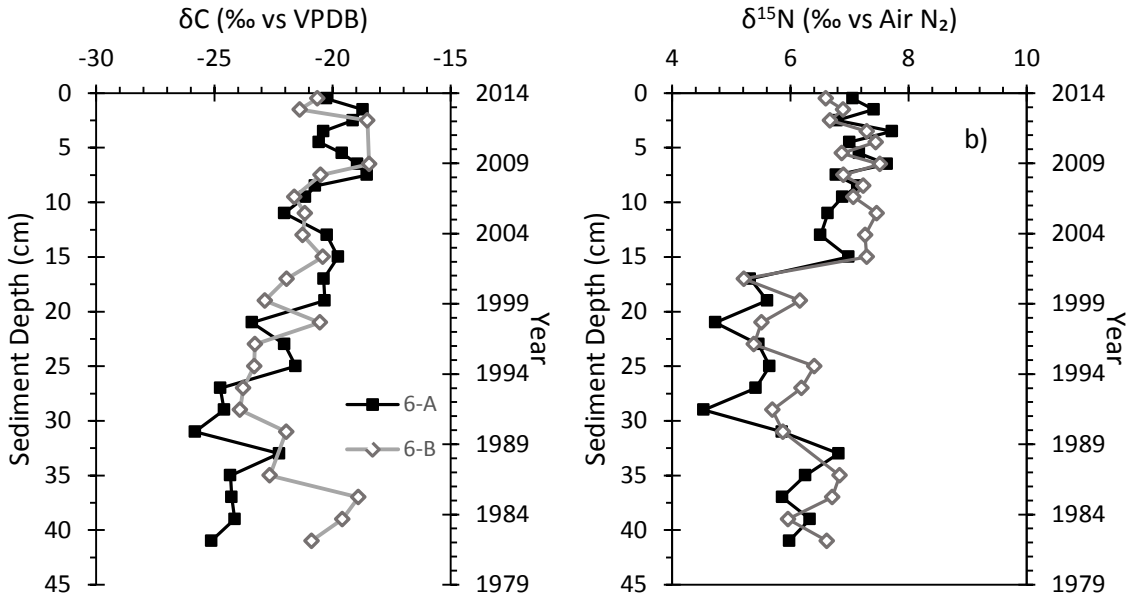

Fig. 7. Stable carbon (panel a) and nitrogen (panel b) isotopic composition of Lake Elsinore sediment relative to standards. Solid squares represent data points in core 6-A. Open diamonds represent data points in core 6-B.

Discussion

Elemental Composition

The organic carbon and total nitrogen concentrations (Fig. 3) increase around the same time that the Lake Elsinore Management Project was completed, surface areas was reduced and mean lake depth increased (Fig. 1b). A greater water depth would have resulted in enhanced organic matter preservation due to increased stratification, less mixing and, thus, more frequent depleted oxygen levels. Another possible explanation for the increase is the amount of organic matter delivered to a given surface area of sediment would have increased when the lake surface area decreased and depth increased. An exponential decrease with depth in the top sediments of organic carbon and nitrogen profiles is generally representative of decomposition (Wetzel, 2001). Sediment at the top of the core has experienced less diagenetic degradation than sediment at 10 cm depth and therefore will contain more organic matter. The fact that OC and N are significantly correlated (Table 1) is further evidence that the decrease is due to decomposition because N is utilized by bacteria during respiration and conversion of organic carbon into CO_2, and N typically decomposes at a similar rate as OC (DiToro, 2001). In addition, water column total N data do not indicate higher concentrations over the past 8-10 years; concentrations vary with no significant trend (Fig. 8). Anderson (2010) indicated that total N content in sediment grab samples (top 10 cm) from fine-textured profundal sediment collected in 2000 and 2010 did not significantly change. This observation further supports the argument that the exponential increase in N toward the top of the sediment is due to degradation processes rather than differences in concentration or loading (Fig. 8).

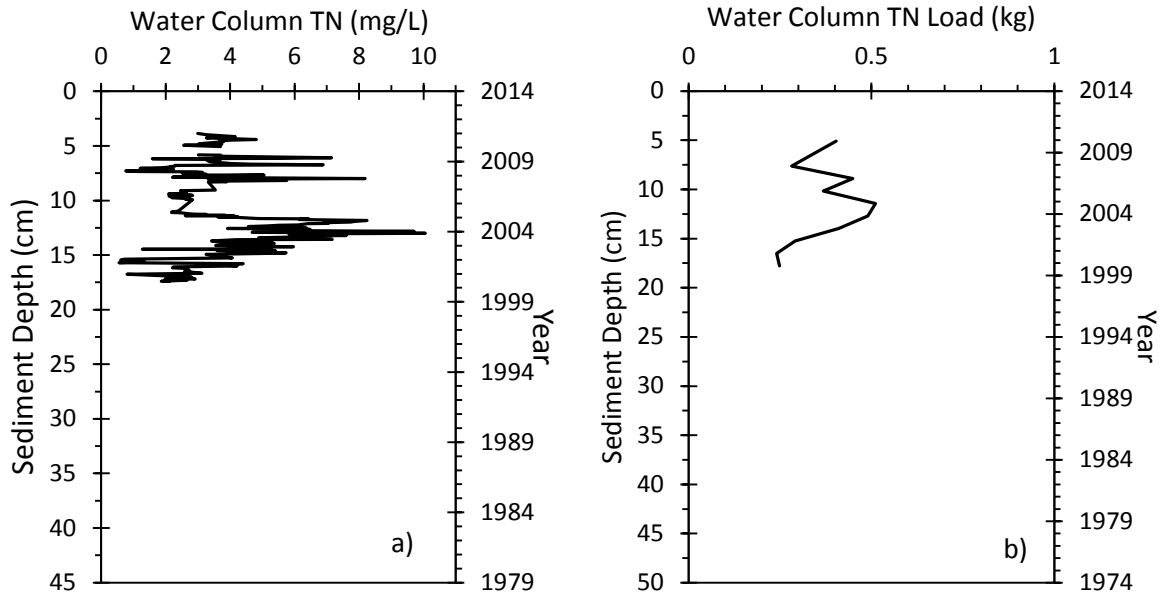

Fig. 8. Average water column total nitrogen concentrations (a) and total nitrogen load (b) in Lake Elsinore.

It is common for C:N of organic matter to increase with depth in the sediment as N is preferentially utilized (Lehman et al., 2002). The fact that OC:N in Lake Elsinore sediment remains approximately constant with depth (Fig. 3) suggests that OM is already highly mineralized in the water column, before it reaches the sediment. The OC:N of suspended organic matter was 6.9, which is 3.1 lower than the sediment, indicating N is selectively recycled as organic matter is settling and/or resuspended. These results are similar to those detected in 2003 in which C and N content of sediment traps was compared to that of the sediment. C and N both decreased from the sediment trap to the sediment and C:N increased from 7.7 to 8.6, indicating greater recycling of N relative to C, although both elements showed evidence of recycling in the water column. From the results of the study, it was concluded that there is substantial recycling occurring on settling particles in the water column (Anderson, 2011). In a study on Lake Simcoe, Canada, in 2011, the deepest bay, Kempenfelt Bay, exhibited constant C:N with sediment depth and this was attributed to the OM being highly recycled in the water column prior to sedimentation (Hiriart-Baer et al., 2011).

Average total TP concentration in Lake Elsinore sediment (0.125% or 1,250 µg/g) (Fig. 3) is consistent with concentrations quantified on other eutrophic lake sediments, which typically range from 1,000 to 1,900 µg/g in surficial sediments (Rydin, 2000; Kapanen, 2012; Dittrich et al., 2013). The depth profile for total phosphorus also reflects an exponential decrease in concentration with sediment depth in the top 10 cm. This exponential decrease in total phosphorus is typical for eutrophic lakes and generally represents mineralization of organic phosphorus (Carey and Rydin, 2011). Fitting an exponential equation to total P concentration in the top 10 cm results in r^2=0.72 and 0.63 for cores 6-A and 6-B respectively, verifying the

exponential trend. We assume that this trend is in fact due to the decomposition of organic matter and not due to increased total phosphorus loading to the lake because organic carbon and TP are significantly correlated in the top 10 cm and the decrease in OC with sediment depth is assumed to be the result of decomposition (see above).

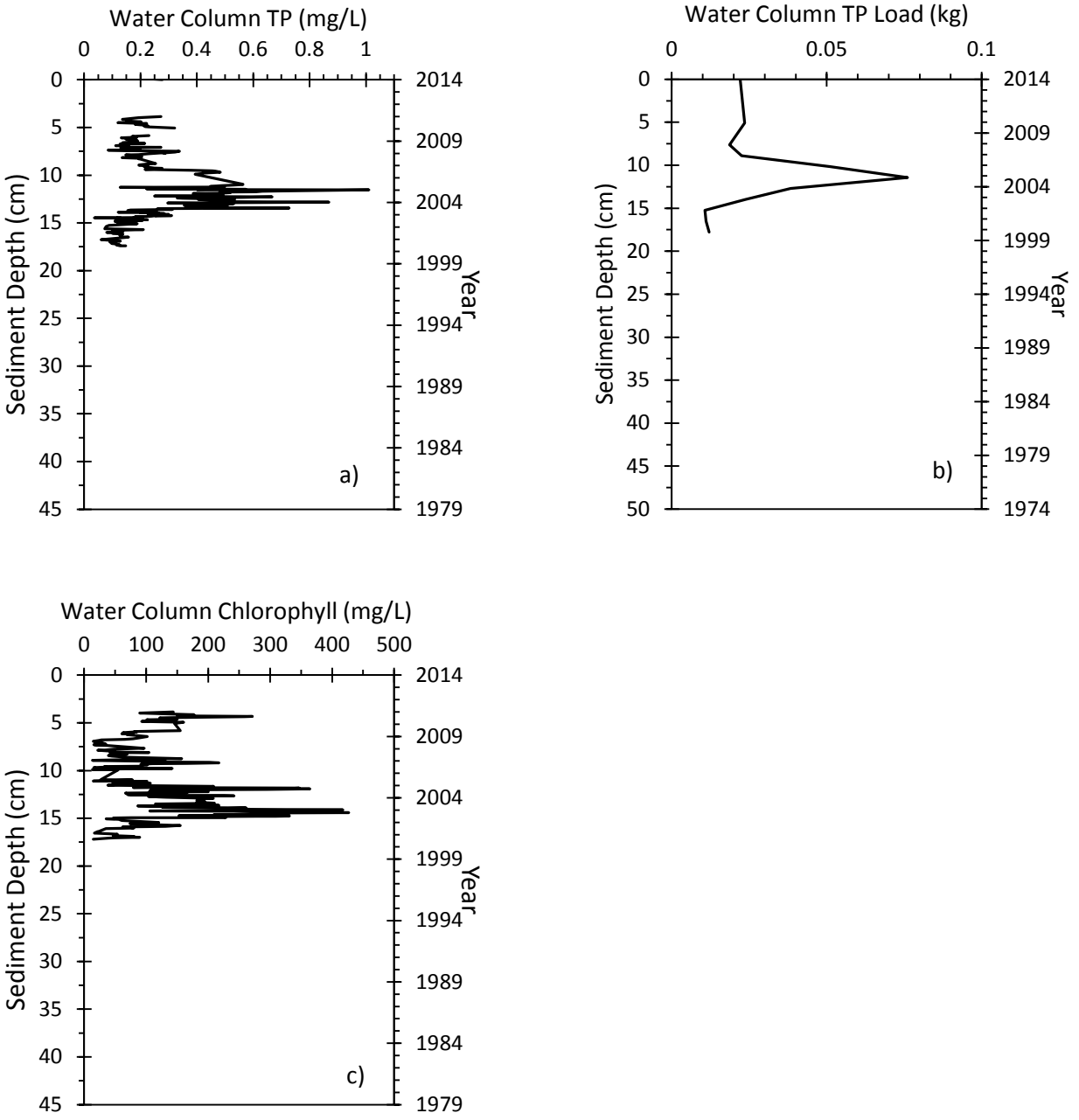

Fig. 9. Average water column a) total phosphorus concentration, b) total phosphorus load, and c) chlorophyll concentrations in Lake Elsinore.

Correlation of total P to OC could in some cases reflect increasing chlorophyll biomass (OC) due to increase in total P loading. However, water column chlorophyll a concentrations in Lake Elsinore do not reflect similar trends (Fig. 9c). Also, external P loading has not been increasing in the past 8-10 years as revealed in the water column TP concentrations from 2000 to 2014 (Fig. 9a). Total phosphorus concentration and load in the water column peaked in 2005 and has been variable since then, rather than exponentially increasing (Anderson, 2010). Anderson (2010) measured a decrease in mean TP concentrations in sediment grab samples from 916 mg/kg in 2000 to 785 mg/kg in 2010, although the difference was not statistically significant. These results further demonstrate that the strongest diagenetic processes are occurring in the surficial sediment. If the increase in TP toward the top of the sediment reflected increased TP concentrations, TP in the grab samples would be expected to increase from 2000 to 2010, not decrease or remain the same. He also concluded that pore-water P concentrations were significantly correlated with organic carbon (r^2 =0.87). A study on a core collected from Lake Elsinore in 2001, however, found that TP was unchanged with depth but that organic P showed an exponential decrease. This difference is interesting, in that it suggests a greater contribution of other P forms to total P in 2001 compared to 2014 (CNRP, 2013).

Calcium and organic carbon are significantly correlated in both cores (Table 1). This correlation suggests calcium carbonate ($CaCO_3$) co-precipitation with organic matter. This process occurs in the epilimnion, when primary production raises the pH, enabling calcite precipitation, and organic matter serves as nuclei for the precipitation (Wetzel, 2001). Anderson (2010) attributed the increase in $CaCO_3$ of sediment grab samples collected from Lake Elsinore from 2000 to 2010 to increased precipitation of calcite in the water column due to erosion of Ca from the watershed in El Niño year 2005 as well as increased productivity and TDS in 2003 and 2004 (Anderson, 2010). The decrease of Ca concentration with depth in the top 10 cm, as well as the correlation with organic carbon, suggests this decrease is due to $CaCO_3$ dissolution coupled to organic matter decomposition (Fig. 4). Respiration leads to increasing carbon dioxide in pore-water which lowers the pH and causes dissolution of $CaCO_3$. Considerable CO_2 concentrations were measured in Lake Elsinore sediments in 2010 (concentrations reaching 3.8±0.6%) which is about 100x atmospheric concentrations, confirming the presence of elevated amounts of CO_2 in pore-water that can contribute to $CaCO_3$ dissolution, the proposed mechanism for decline in Ca with depth (Anderson, 2010). Similar to OC and N (Fig. 3), calcium concentrations increase around the year 1994 due to increased preservation of OC, which is precipitated with Ca, resulting in increased preservation of Ca as well (Fig. 4).

In order to confirm that diagenesis is the driving force for the decreasing trends in the top 10 cm of OC, N, TP, and Ca profiles, the data was fit to an exponential function, because organic matter decomposition is an (exponential) first order decay process (Wetzel, 2001).

$$C_t = C_0 e^{-kt} \qquad (3)$$

Fitting the data to an exponential function also enables the calculation of the rate constants, depicting the rate of mineralization, or loss of the element. In the equation above, k is the slope of the function and represents rate change per depth in the sediment with units of

cm^{-1}. To calculate the rate per time, k_r, the k is multiplied by sedimentation rate. Once k is calculated, half-life can be calculated following the equation below. Rate constants for the exponential decline in OC, N, and TP concentrations in the top 10 cm with depth were calculated to confirm diagenesis is the driving force for these trends. Rate constants for each element were averaged between the two replicate cores and that average was used to calculate half-life, using the equation:

$$t_{1/2} = 0.693/k_r \quad (4)$$

The exponential fit to OC was statistically significant at p=0.001 with r^2=0.73 and 0.76. The exponential fit to N was statistically significant at 0.01 but the goodness of fit wasn't as strong, with r^2=0.68 and 0.72 (for 6-B p=0.001). TP fit the exponential function at p=0.001 with r^2=0.79 and 0.64 (p=0.01). This discrepancy may have skewed the TP average half-life. For 6-A the calculated half-life was 21.5 years and for 6-B the half-life was 12.16 years, yielding an average of 15.4 years (Table 1), although it may be a little longer than that, due to 6-A (half-life 21.5 years) demonstrating a better fit to the exponential function. The exponential fit to calcium in Lake Elsinore sediment was significant at 0.001 with r^2=0.9 and 0.81. The goodness of fit for calcium was greater than the other three elements. The significance of the goodness of fit of each element to an exponential function indicates that the decrease in depth can be attributed to sedimentary diagenesis, or decomposition.

The rate constants for OC an N were slightly greater than those for TP and Ca, suggesting that OC and N mineralize at about 1.5x the rate than TP and Ca, indicating that OC and N do not remain bioavailable for as long as TP and Ca. OC and N had very similar rate constants and therefore very similar half-lives, of about 10 years (Table 3). These values are lower from the half-life for OC and N determined on a core collected in 2001, which were calculated to be 24 and 30 years, respectively, using a 1-phase model, but similar to the half-lives calculated using a 2-phase model (Anderson, 2011). In the present analysis, the uppermost 10 cm was fitted, while the 2-phase model represented labile recently deposited material as well as an older less reactive phase. The 95% upper and lower confidence intervals represent the error in fitting the data to an exponential curve (Table 3). The half-lives calculated for the upper and lower rate constants confidence intervals were about 18 and 6.5.

The half-lives for calcium and total phosphorus were similar, at around 15 years. This similarity further corroborates the concept of $CaCO_3$ dissolution with increasing sediment depth due to decreasing pH and subsequent SRP and Ca^{2+} release to pore-water. The average half-life for total phosphorus was 15.4 years, but the error was greater than that for OC and N. Similar to the results from calculations for organic phosphorus from 2001, TP had a rate constant that was lower than those for OC and N, indicating slower mineralization and longer period of recycling of P in the sediment. However, taking error estimates into consideration, the half-life for TP calculated in this study (15.4 yrs, with upper confidence interval of 37.2 yrs) is about half of that calculated for organic P in 2001 using a 2-phase model (29.7 years) (Anderson, 2011). Notwithstanding, the large uncertainty in the calculated half-life for total P (95% CI of 7.8 – 37.2 yrs) and comparison between values calculated for total P in this study

and organic-P in Anderson (2001) make it difficult to draw any firm conclusions between sediment cores collected in 2001 and 2014.

Table 3. Rate constants and half-lives for organic carbon, total nitrogen, total phosphorus, and calcium.

	k_r (yr^{-1})	$t_{1/2}$ (yr^{-1})	Upper 95% C.I.	Lower 95% C.I.
Organic Carbon	0.066±0.003	10.5	18.8	6.9
Total Nitrogen	0.073±0.0	9.5	17.8	6.3
Total Phosphorus	0.045±0.018	15.4	37.2	7.8
Calcium	0.046±0.003	15.1	24.9	11.5

The iron content of sediments decreases from 6.2% prior to 1990 to 5.8% by about 1994 and then is constant until about 2006, before declining more recently (Fig. 5). Similarly, sulfur (S) increases in 1994 and is constant to the top of the core (Fig. 4). Following completion of LEMP in 1994/1995, lake depth increased and presumably there was less circulation and less DO reaching the sediment surface and hypolimnion. This would lead to chemical reduction of iron and sulfate and cause precipitation of FeS, which may explain why the two elements exhibit similar trends during this time. Prior to this time, the redox conditions may have resulted in iron reduction and release to the water column but the redox conditions were not low enough to enable sulfate reduction until the lake deepened. Iron increases with depth in the top 10 cm due to increasing precipitation of FeS with depth, as more and more sulfate is reduced during organic matter decomposition. According to Wakefield (2001), sulfate concentrations in Lake Elsinore pore-water decreased with depth and sulfide concentrations increased which she attributed to increased FeS precipitation with depth as sulfate reduction takes place (greater with depth because DO in sediment decreases with depth). This iron then becomes locked up and is no longer able to bind to P.

The increase in silicon and aluminum concentrations between 25 and 30 cm in core 6-A corresponds to the time period when the Lake Elsinore Management Project was in progress (Fig. 4). Levee construction and construction of a new inlet and outlet channel would have resulted in increased erosion and dredging, causing a large influx of inorganic particles (silt and clay minerals) to the sediment, although this was not observed in core 6-B. The transition from a large and shallow mean depth lake to a deeper mean depth lake, however, did not result in lasting changes to these elements' concentrations in the sediment, as after 1995, concentrations returned to background levels.

Correlation analysis comparing sediment properties with sources of inflow and physical hydrologic characteristics of the lake revealed a few notable significant relationships at $p<0.05$ (Table 4; Table 5). The correlation between local runoff and aluminum, silicon, potassium, titanium, and iron reflects erosional inputs to the lake from the surrounding watershed during precipitation events (Table 4). The significant negative correlation of organic carbon, nitrogen, and calcium with local runoff suggests dilution of organic constituents corresponding to an influx

of large amounts of inorganic elements in local runoff (Table 4). In comparison, inflow from the San Jacinto River exhibits weaker, non-significant relationships with elements, which can be attributed to sediment trapping in upstream Canyon Lake (Table 4). Recycled water inputs appear to be significantly correlated with OC and N, suggesting contribution to organic matter production in the lake through increased nutrient inputs in wastewater, although diagenetic processes operating over this same timeframe complicate interpretation of these r-values. Given the small n-size and importance of diagenesis, no clear conclusion can be drawn from this simple statistical calculation.

Table 4. Correlation table showing r values for hydrologic properties and inflows to Lake Elsinore for period 1981-2014 (entire core length). With n=26, an r value of 0.38 is statistically significant at $p<0.05$, and 0.51 is statistically significant at $p<0.001$. USGS data from gage #11070500.

Property	Avg. Area	SJ Inflow	Local Runoff	Recycled H_2O	Avg. Elev.
δ 13C	-0.14	-0.19	-0.30	0.50	-0.07
δ15N	-0.24	-0.23	-0.55	-0.63	-0.16
%OC	-0.22	-0.16	-0.42	0.89	0.01
%N	-0.27	-0.16	-0.44	0.82	-0.06
Al-P	0.04	0.22	0.16	-0.08	0.08
Mobile-P	-0.10	-0.05	0.14	-0.12	-0.25
Al	0.20	0.36	0.43	-0.16	-0.48
Si	0.22	0.36	0.43	-0.15	-0.48
P	-0.30	-0.22	-0.39	0.27	-0.76
S	-0.21	0.12	-0.18	-0.07	-0.26
K	0.38	0.12	0.49	-0.41	0.61
Ca	-0.41	-0.29	-0.62	0.55	0.78
Ti	0.33	0.11	0.50	-0.55	-0.81
Fe	0.30	0.17	0.49	-0.46	-0.71

Phosphorus Forms

The average concentration of loosely-sorbed/pore-water P in Lake Elsinore (125 µg/g) is greater than many other studied eutrophic lakes, including Lake Peipsi, Estonia (11 µg/g) and Lake Erken, Sweden (53 µg/g) (Rydin, 2000; Kapanen, 2012). Generally in eutrophic lakes, mobile P (specifically loosely-sorbed/pore-water P) will increase toward the sediment surface which indicates diffusion toward the water column (Rydin, 2000). However, in such a shallow lake as Lake Elsinore, with bioturbation and strong bottom shear during periods of high wind speeds, diffusion may be very rapid, such that a concentration gradient toward the sediment surface is not depicted in the profiles (Fig. 6). In addition, the ebullition of CH_4 gas bubbles generated by microbes can stimulate the diffusion of P toward the water column (Wetzel, 2001, Kapanen, 2012). Martinez and Anderson (2013) measured elevated levels of CH_4 gas in the

sediment and ebullition at numerous sites on Lake Elsinore, including site 6 where cores were collected.

The high concentrations of loosely-sorbed (NH_4Cl-extractable) P and relatively low concentrations of iron-bound P in Lake Elsinore sediment are unusual compared to other lakes in the region (Table 5), and eutrophic lakes more generally which exhibit very little contribution of loosely-sorbed phosphate to mobile P (Pilgrim et al., 2007). In the Lake Elsinore sediment cores, NH_4Cl-P averaged about 120 µg/g and 63% of the mobile-P in the upper 10 cm, while Fe-P averaged about 70 µg/g (Table 5). In Big Bear Lake, a mesotrophic lake also located in the San Bernardino mountains, only 1 µg/g NH4Cl-extractable P was present in the sediments, with essentially all (99%) of the mobile-P of surface sediments there present as a reducible Fe-P phase. Canyon Lake, the reservoir located upstream from Lake Elsinore, contains 5x greater Fe-P (average of 386 µg/g and 87% of mobile-P) than Lake Elsinore and one-half the amount of NH_4Cl-extractable P (Table 5). The disparity between Fe-P in Lake Elsinore compared with other lakes in the region and with many other eutrophic lakes may be explained by a low influx of iron to the lake due to sedimentation of particulate iron within Canyon Lake.

Table 5. Comparison of concentrations of P in different forms within sediments of selected lakes in Southern California.

Lake	**Mean Phosphorus Fractionation in Sediments (µg g^{-1} dw)**			
(n=# sites)	**NH_4Cl-P**	**Fe-P**	**Mobile-P**	**NaOH (Al)-P**
Big Bear L. (n=15)	1 (1%)	129 (99%)	130	191
Canyon L. (n=5)	59 (13%)	386 (87%)	459	890
L. Elsinore (n=2)	120 (63%)	70 (37%)	190	150
Diamond Valley L (n=20)	1 (1%)	91 (99%)	92	268

The increased amount of Al-P in lake sediment around a depth of 25 cm is reflected in aluminum and silicon profiles and corresponds approximately to 1994 which is around the time of completion of the LEMP. The construction involved in the project likely increased suspension, erosion and deposition of inorganic particles to the sediment and increased precipitation of aluminum-bound phosphate (see Elemental Composition discussion above).

Stable Isotopic Composition

The gradual increase in $\delta^{13}C$ toward the top of the sediment core (Fig. 7) may result from either diagenetic processes or from increasing eutrophic conditions in the lake. Diagenetic processing of organic matter in the sediment typically accounts for a decrease of 1.6-1.8‰ due to selective decomposition of enriched carbohydrates and proteins, which are easier to degrade, as well as the addition of depleted microbial biomass (Lehmann et al., 2002). A study on Lake Lugano found that sediment was depleted by 1.5‰ compared to sediment traps corresponding to the same time (Lehmann et al., 2002). However, suspended organic matter bore a $\delta^{13}C$ of -20‰, which is the same as the sediment. If OC is being degraded in the water column, as evidenced in Anderson (2010), then this indicates that at least during early diagenesis, there is

very little fractionation effect or change on $\delta^{13}C$ values. The decomposed suspended organic matter resulted in a $\delta^{13}C$ of -23.7‰, which indicates a -3.7‰ shift during diagenesis. However, because this SOM spent an unknown amount of time incubating under room temperature, it may have undergone more decomposition than SOM typically would in Lake Elsinore before sedimentation and permanent burial (less prone to decay with increased burial).

Increasing eutrophication has also been determined to lead to increases in $\delta^{13}C$ of sediment. A study of three Florida lakes of different trophic levels reported that $\delta^{13}C$ was lowest in the oligotrophic lake and highest in the eutrophic lake and that in the hypereutrophic lake, Lake Apopka, $\delta^{13}C$ increased up-core from -23 to -18 (Torres et al., 2012), which is approximately the same magnitude increase as in the Lake Elsinore sediment (Fig. 7). A study on Lake Ontario found a progressive increase in $\delta^{13}C$ of organic matter with increasing phosphorus loading and water column P concentrations, which also supports the hypothesis that $\delta^{13}C$ reflects lacustrine productivity. In that study, $\delta^{13}C$ increased from -27 to -25. A significant correlation between organic carbon and calcium carbonate was observed in Lake Ontario as well, which suggests photosynthesis generated calcite co-precipitation increases the sedimentation of organic matter and enhances its preservation in the sediment (Hodell and Schelske, 1998). If this is the case in Lake Elsinore, diagenesis may only be affecting $\delta^{13}C$ for a short period of time before permanent burial preserves the $\delta^{13}C$ signature of organic matter. Without water quality data dating back to the early 1980s, it is difficult to determine whether the increasing trend in $\delta^{13}C$ toward the top of the core is due to increasing primary production or simply reflects sedimentary diagenesis.

The $\delta^{15}N$ results reflect three distinct periods in Lake Elsinore's recent history. The section at bottom of the core from 41 to 35 cm corresponds to the period of time when the lake was shallow, with presumably greater circulation and mixing. The transition to a deeper lake with the completion of the Lake Elsinore Management Project resulted in a decrease in sedimentary $\delta^{15}N$. The reason for this decline lies predominantly in the fact that increased lake depth led to a decrease in circulation and increase in stratification and anoxia. With the completion of the Lake Elsinore Management Project and resulting increase in lake depth, nitrate-nitrogen would have been less available than ammonium, and increasing incorporation of ammonium by phytoplankton could have resulted in the decrease in $\delta^{15}N$. During assimilation, phytoplankton fractionate ammonium by about -10‰ and nitrate by -1 to -3.4‰, so increased ammonium uptake relative to nitrate-nitrogen would result in a decline in $\delta^{15}N$ of algal biomass (Teranes and Bernasconi, 2000; Lu et al., 2010). Also, the majority of NH_4 is generated from organic matter mineralization in which ^{14}N is preferentially mineralized over ^{15}N during organic matter hydrolysis so ammonium is more depleted in ^{15}N than nitrate even before uptake by phytoplankton (Torres et al., 2012; Lehmann et al., 2002).

In addition to an increased utilization of ammonium over nitrate, during oxic decomposition of algal biomass, there is typically very little change in $\delta^{15}N$, but during anoxic decay (in the sediments or anoxic bottom water), $\delta^{15}N$ typically decreases by 2.5 to 4‰ due to the input of depleted microbial biomass (Lehmann et al., 2002). Bacterial growth and

consumption of the depleted ammonium from decomposition in addition to fractionation during bacterial excretion of ammonia which preferentially excretes ^{15}N leads to the depletion of $\delta^{15}N$ of bacterial biomass (Lehmann et al., 2002). When there is a large amount of bacterial growth and activity in the sediment, as is usually the case in stratified lakes with anoxic bottom water, it can cause a reduction in the $\delta^{15}N$ of sediment (Lehman et al., 2002).

Increasing autochthonous productivity can lead to increases in sedimentary $\delta^{15}N$ signatures when phytoplankton become more enriched in ^{15}N. However, this only occurs if surface waters become depleted in N, which typically only happens if a lake is nitrogen-limited (Torres et al., 2012; Teranes et al., 2000). Analysis of sedimentary $\delta^{15}N$ in Lake Simcoe, a eutrophic lake in Canada, revealed an up-core increase from 4.5‰ to 7.3‰ due to increasing productivity (Hiriart-Baer et al., 2011). The N:P in the water column in Lake Elsinore (17.4) indicates that Lake Elsinore is generally not N-limited and water column concentrations of TN do not wane in recent years, therefore the increase to higher $\delta^{15}N$ values around 2002 cannot be attributed to changes in N loading and availability in the water column (Fig. 8) (CNRP, 2013).

The shift to higher $\delta^{15}N$ values around the year 2002 is more likely due to the input of supplemental wastewater. Sewage, composed of human and animal waste, has nitrate with $\delta^{15}N$ between 10 and 20‰. Nitrate input from soils and terrestrial organic matter in the watershed has values between 2-5‰ while fertilizers exhibit lower $\delta^{15}N$, approximately 3‰ (Teranes and Bernasconi, 2000; Machiwa, 2010; Torres et al., 2012). Assuming a $\delta^{15}N$ value of 3‰ for nitrate input from local runoff and San Jacinto River inflow and a value of 15‰ for nitrate input from recycled wastewater, one can calculate predicted $\delta^{15}N$ values of Lake Elsinore sediment. Using assumed N isotope signatures for each source of water to the lake as well as average annual inflow (2008-present) of 10,000 acre-feet from local runoff/San Jacinto River and 5,600 acre-feet from recycled wastewater, the predicted $\delta^{15}N$ value is calculated as 7.37‰. The actual $\delta^{15}N$ at site 6 in Lake Elsinore was on average 7.12‰ from 2001 to present which is very similar to the predicted value with a 3.5% error.

Denitrification in the water column also results in $\delta^{15}N$ enrichment of the sediment because denitrification preferentially reduces ^{14}N over ^{15}N, leaving residual nitrate enriched in ^{15}N (Teranes and Bernasconi, 2000; Lu et al., 2010). In Lake Ontario, Canada, an increase in $\delta^{15}N$ of 0.3‰ over a period of ten years, and subsequent stabilization of $\delta^{15}N$ were attributed to denitrification (Hodell and Schelske, 1998). Prior to wastewater additions, denitrification rates in the water column were fairly low due to low concentrations of nitrate (Horne, 2009). Therefore, wastewater input may be enabling denitrification by providing NO_3 for the reaction. Denitrification is likely occurring in the water column near the sediment-water interface because sedimentary denitrification does not result in a fractionation effect and $\delta^{15}N$ of suspended organic matter (5.8‰) was lower than the surficial sediment values, indicating that denitrification is occurring in the benthic boundary layer or bottom of the water column prior to permanent sedimentation (Terranes and Bernasconi, 2000). Another reason that suspended organic matter is more depleted in $\delta^{15}N$ than sediment is that as it is settling, OM degradation results in enrichment of residual OM as ^{14}N ammonium is preferentially released (Torres et al., 2012;

Lehmann et al., 2002). The suspended organic matter sample that experienced decomposition resulted in a $\delta^{15}N$ of 10‰, which is greater than the top sediment isotopic signature. This discrepancy suggests that the algal biomass experienced greater decay than it would have in the lake, where it would be progressively buried in the sediment (N recycling decreases with increasing sediment depth, see Elemental Composition section above).

Conclusions

The isotopic and elemental analysis of sediment cores from Lake Elsinore provided new insights into the depositional history and biogeochemical cycling of organic matter and nutrients in this eutrophic lake:

(i) organic matter is highly mineralized in the water column prior to permanent sedimentation;

(ii) the transition from shallow to deeper lake with the completion of LEMP resulted in increased organic matter preservation in the sediment, evidenced by an increase in OC, N, Ca, and S during this time;

(iii) a lack of correlation between iron and phosphorus, yet significant correlation between phosphorus and organic carbon and calcium in the top 10 cm suggests P cycling is controlled by calcium and organic matter rather than redox conditions and corresponding Fe geochemistry;.

(iv) fitting exponential functions to OC, TN, TP, and calcium data revealed that their decline with sediment depth is due to diagenetic processes rather than changes in water column concentrations.

(v) Lake Elsinore sediments have much higher concentrations of NH_4Cl-extractable P and lower Fe-P than other lakes in the region, with dramatically different values than Canyon Lake that are attributed to retention of particulate Fe and Al phases in Canyon Lake;

(vi) $\delta^{15}N$ values in sediment declined with completion of LEMP and the corresponding average increased mean depth of the lake;

(vii) $\delta^{15}N$ values in sediment subsequently increased due to wastewater input and denitrification.

References

Anderson, Michael A. 2010. *Bathymetric, Sedimentological and Retrospective Water Quality Analysis to Evaluate Effectiveness of the Lake Elsinore Recycled Water Pipeline Project.* Final Report Submitted to Lake Elsinore and San Jacinto Watersheds Authority.

Anderson, Michael A. 2011. Task 1: *Estimate Rate at Which Phosphorus is Rendered No Longer Bioavailable in Sediments.* Technical Memorandum submitted to Lake Elsinore and San Jacinto Watersheds Authority

American Public Health Association. 1998. *Standard Methods for the Examination of Water and Wastewater*. 20th Edition: 4-148-149.

Byrne, Roger, Matthew Kirby, Steve Lund, Liam Reidy, and Christopher Poulson. 2004. Changing Sedimentation Rates during the Last Three Centuries at Lake Elsinore, Riverside County, California. Final Report to the Santa Ana Regional Water Quality Control Board, Riverside, CA. 41pp.

California Environmental Protection Agency, Santa Ana Regional Water Quality Control Board. (1995). Water Quality Control Plan for the Santa Ana River Basin (Region 8). January 24, 1995. Updated February 2008. Accessed from California Environmental Protection Agency website http://www.swrcb.ca.gov/santaana/water_issues/programs/basin_plan/index.shtml

Carey, Cayelan C., and Emil Rydin. 2011. Lake trophic status can be determined by the depth distribution of sediment phosphorus. *Limnology & Oceanography* 56 (6): 2051-2063.

City of Lake Elsinore. 2006. Water Resources Background Report as part of the Lake Elsinore General Plan. Retrieved from lake-elsinore.org

Dean, Walter E. 2006. Characterization of Organic Matter in Lake Sediments from Minnesota and Yellowstone National Park. Report 2006-1053. Open-File Report. USGS Publications Warehouse. http://pubs.er.usgs.gov/publication/ofr20061053.

DiToro, Dominic M. 2001. *Sediment Flux Modeling*.

Dittrich, M., A. Chesnyuk, A. Gudimov, J. McCulloch, S. Quazi, J. Young, J. Winter, E. Stainsby, and G. Arhonditsis. 2013. Phosphorus Retention in a Mesotrophic Lake under Transient Loading Conditions: Insights from a Sediment Phosphorus Binding Form Study. *Water Research* 47 (3): 1433–47.

Egemose, Sara, Kasper Reitzel, Frede Ø. Andersen, and Henning S. Jensen. 2013. Resuspension-Mediated Aluminium and Phosphorus Distribution in Lake Sediments after Aluminium Treatment. *Hydrobiologia* 701 (1): 79–88.

Elsinore Valley Municipal Water District (EVMWD). http://www.evmwd.com/about/departments/public/lake.asp

Fry, Brian. 2006. *Stable Isotope Ecology*. Springer Science+Business Media, LLC.

Gälman, Veronika, Johan Rydberg, and Christian Bigler. 2009. Decadal Diagenetic Effects on δ13C and δ15 N Studied in Varved Lake Sediment. *Limnology & Oceanography* 54 (3): 917–24.

Hiriart-Baer, Véronique P., Jacqui Milne, and Christopher Marvin, 2011. Temporal trends in phosphorus and lacustrine productivity in Lake Simcoe inferred from lake sediment. *Great Lakes Research* 37: 764-771.

Hodell, David A., and Claire L. Schelske. 1998. Production, Sedimentation, and Isotopic Composition of Organic Matter in Lake Ontario. *Limnology and Oceanography* 43 (2): 200–214.

Horne, Alex J. 2009. Three Special Studies on Nitrogen Offsets in Semi-Desert Lake Elsinore in 2006-08 as part of the nutrient TMDL for reclaimed water added to stabilize lake levels. Retrieved from SAWPA: http://www.sawpa.org/wp-content/uploads/2012/09/HORNEN-OFFSETSRptDrafttoEVMWD6_001.pdf

Hudson, Tom. (City of Lake Elsinore, City Timeline) retrieved from lake-elsinore.org.

Hupfer, Michael, Dominik Zak, Reingard Roßberg, Christiane Herzog, and Rosemarie Pöthig. 2009. Evaluation of a Well-Established Sequential Phosphorus Fractionation Technique for Use in Calcite-Rich Lake Sediments: Identification and Prevention of Artifacts due to Apatite Formation. *Limnology and Oceanography: Methods* 7: 399–410.

Jan, Jiří, Jakub Borovec, Jiří Kopáček, and Josef Hejzlar. 2013. What Do Results of Common Sequential Fractionation and Single-Step Extractions Tell Us about P Binding with Fe and Al Compounds in Non-Calcareous Sediments? *Water Research* 47 (2): 547–57.

Jankowski, KathiJo, Daniel E. Schindler, and Gordon W. Holtgrieve. 2012. Assessing Nonpoint-Source Nitrogen Loading and Nitrogen Fixation in Lakes Using δ15N and Nutrient Stoichiometry. *Limnology & Oceanography* 57 (3): 1–1.

Kapanen, Galina. 2012. Pool of Mobile and Immobile Phosphorus in Sediments of the Large, Shallow Lake Peipsi over the Last 100 Years. *Environmental Monitoring and Assessment* 184 (11): 6749–63.

Kleeberg, Andreas, Christiane Herzog, and Michael Hupfer. 2013. Redox Sensitivity of Iron in Phosphorus Binding Does Not Impede Lake Restoration. *Water Research* 47 (3): 1491–1502.

Lake Elsinore/Canyon Lake TMDL Task Force. 2007. In-Lake Sediment Nutrient Reduction Plan for Lake Elsinore. Retrieved from http://www.swrcb.ca.gov/rwqcb8/water_issues/programs/tmdl/docs/elsinore/implemetation/Lake_Elsinore_Sediment_Nutrient_Reduction_Plan_10-22-07.pdf

Lake Elsinore/Canyon Lake TMDL Task Force. 2010. Lake Elsinore & Canyon Lake Nutrient TMDL Annual Water Quality Report. Final Report prepared for Santa Ana Regional Water Quality Control Board.

Lehmann, Moritz F, Stefano M Bernasconi, Alberto Barbieri, and Judith A McKenzie. 2002. Preservation of Organic Matter and Alteration of Its Carbon and Nitrogen Isotope Composition during Simulated and in Situ Early Sedimentary Diagenesis. *Geochimica et Cosmochimica Acta* 66 (20): 3573–84.

Lu, Yuehan, Philip A. Meyers, Thomas H. Johengen, Brian J. Eadie, John A. Robbins, and Haejin Han. 2010. $\delta^{15}N$ Values in Lake Erie Sediments as Indicators of Nitrogen Biogeochemical Dynamics during Cultural Eutrophication. *Chemical Geology* 273 (1/2): 1–7.

Machiwa, John F. 2010. Stable Carbon and Nitrogen Isotopic Signatures of Organic Matter Sources in near-Shore Areas of Lake Victoria, East Africa. *Journal of Great Lakes Research* 36 (1): 1–8.

Martinez, D. and M.A. Anderson. 2013. Methane production and ebullition in a shallow, artificially aerated, eutrophic temperate lake (Lake Elsinore, CA). *Sci. Total Environ.* 454-455:457-465.

Moosmann, Lorenz, René Gächter, Beat Müller, and Alfred Wüest. 2006. Is Phosphorus Retention in Autochthonous Lake Sediments Controlled by Oxygen or Phosphorus? *Limnology and Oceanography* 51 (1_part_2): 763–71.

Pilgrim, Keith M., Brian J. Huser, and Patrick L. Brezonik. 2007. A Method for Comparative Evaluation of Whole-Lake and Inflow Alum Treatment. *Water Research* 41 (6): 1215–24.

Riverside County Flood Control & Water Conservation District. 2013. Comprehensive Nutrient Reduction Plan for Lake Elsinore and Canyon Lake. CDM Smith Consulting.

Rydin, E. 2000. Potentially Mobile Phosphorus in Lake Erken Sediment. *Water Research* 34 (7): 2037–42.

Søndergaard, Martin, Jens Peder Jensen, and Erik Jeppesen. 2003. Role of Sediment and Internal Loading of Phosphorus in Shallow Lakes. *Hydrobiologia* 506-509 (1-3): 135–45.

Teranes, Jane L., and Stefano M. Bernasconi. 2000. The Record of Nitrate Utilization and Productivity Limitation Provided by $\delta^{15}N$ Values in Lake Organic Matter-A Study of Sediment Trap and Core Sediments from Baldeggersee, Switzerland. *Limnology and Oceanography* 45 (4): 801–13.

Torres, Isabela C., Patrick W. Inglett, Mark Brenner, William F. Kenney, and K. Ramesh Reddy. 2012. Stable Isotope (δ13C and δ15N) Values of Sediment Organic Matter in Subtropical Lakes of Different Trophic Status. *Journal of Paleolimnology* 47 (4): 693–706.

U.S. Geological Survey. USGS Current Conditions for the Nation. Site #11070500, San Jacinto R NR Elsinore. http://waterdata.usgs.gov/nwis/uv?

Victoria, Reynaldo Luiz, Luiz Antonio Martinelli, Paulo C. O. Trivelin, Eiichi Matsui, Bruce R. Forsberg, Jeffrey E. Richey, and Allan H. Devol. 1992. The Use of Stable Isotopes in Studies of Nutrient Cycling: Carbon Isotope Composition of Amazon Varzea Sediments. *Biotropica* 24 (2): 240–49.

Vreca, Polona, and Gregor Muri. 2006. Changes in Accumulation of Organic Matter and Stable Carbon and Nitrogen Isotopes in Sediments of Two Slovenian Mountain Lakes (Lake Ledvica and Lake Planina), Induced by Eutrophication Changes. *Limnology & Oceanography* 51 (1): 781–90.

Wakefield, Elisha Marie. 2001. *Internal Loading of Nutrients in Three Southern California Lakes*.

Wetzel, Robert. 2001. *Limnology: Lake and River Ecosystems*. Third Edition. Elsevier Academic Press.

Widerlund, Anders, Sara Chlot, and Björn Öhlander. 2014. Sedimentary Records of δ13C, δ15N and Organic Matter Accumulation in Lakes Receiving Nutrient-Rich Mine Waters. *Science of the Total Environment* 485-486 (July): 205–15.

Technical Memorandum

Task 2.2: Fishery Hydroacoustic Survey and Ecology of Lake Elsinore: Spring 2015

Objective

The objective of this task was to quantify the fishery in Lake Elsinore for comparison with earlier survey results. A limited sampling of the phytoplankton and zooplankton communities was also conducted.

Approach

Zooplankton were sampled on March 7, 2015 near the deep-water site (site 6 or E2) and near the San Jacinto River channel/ski school site via vertical tows with an 80 µm Wisconsin net. Samples were preserved with 70% ethanol in the field, returned to the laboratory and inspected under Nikon compound and dissecting microscopes. Approximately 250 individuals were inspected and counted from each site. Water samples were also collected at about 0.3 m depth into 125 mL polypropylene bottles at the 2 sites, returned to the laboratory and the phytoplankton community was inspected under a Nikon compound microscope. Total dissolved solid (TDS) concentrations of the water samples were calculated from measured electrical conductance values.

A hydroacoustic survey was conducted on April 2, 20125 to quantify the fishery in the lake for comparison with earlier survey results. The survey was conducted using a BioSonics DT-X echosounder with a 201-kHz split beam transducer. Data were acquired at 5 pps. The transducer was calibrated using a tungsten-carbide calibration sphere in the field prior to collection of acoustic data and at the end of the day's survey. Echograms were analyzed using BioSonics VisualAnalyzer.

Results

Lake level and TDS

Four years of drought had substantially lowered the level of Lake Elsinore; surface elevation was approximately 1236.6 ft above MSL at the time of these measurements in spring 2015. The TDS concentrations reached 2700 mg/L which were the highest since regular monitoring began in 2000. This value exceeded the previous high of about 2300 mg/L in late 2003.

Phytoplankton

Transparency of the lake was very poor throughout the spring and summer of 2015, with Secchi depth values <10 – 15 cm throughout this period. The poor clarity resulted from excessive amounts of phytoplankton in the water column, with the phytoplankton community strongly dominated (>95%) by the filamentous blue-green algae *Pseudanabaena* (formerly *Oscillatoria*). This phytoplankton dominated the

community during the very poor transparencies and very high chlorophyll a concentrations observed in 2002-2004, but was also the dominant phytoplankton during the summer of 2010 as well, when Secchi depths averaged 30 - 40 cm (*P. limnetica* comprised 75-90% of biomass in June-August 2010) (Anderson et al., 2011). This species appears to have a unique adaptation to shallow, relatively well-mixed high TDS conditions at Lake Elsinore. The species is also a poor food resource for filter-feeding *Daphnia* and other large-bodied cladocera, since the filaments are too large to enter the mouth and further interfere with filtration of smaller phytoplankton.

Zooplankton

A total of 489 individuals were inspected and counted from the two sites sampled on March 7, 2015. Adult copepods dominated the zooplankton community, comprising 83.8% of the total individuals counted (Table 1; Fig. 1a,b). Juvenile copepods (nauplii) were the second most abundant group of zooplankton at 14.7% of the community (Table 1; Fig 1a). Rotifers were absent at site 6, although 4 individuals were identified in the sample collected near the San Jacinto River inlet site (Table 1). A single *Daphnia* was present in the samples (Fig. 1c), corresponding to a relative abundance of 0.2% within the zooplankton community. Also depicted in Fig. 1 as small filaments are *Pseudanabaena.*

Table 1. Zooplankton community in Lake Elsinore: March 7, 2015.

Site	Copepods	Nauplii	Rotifers	*Daphnia*	Total
SJR Inlet	180	55	4	1	242
Site 6 (E2)	230	17	0	0	247

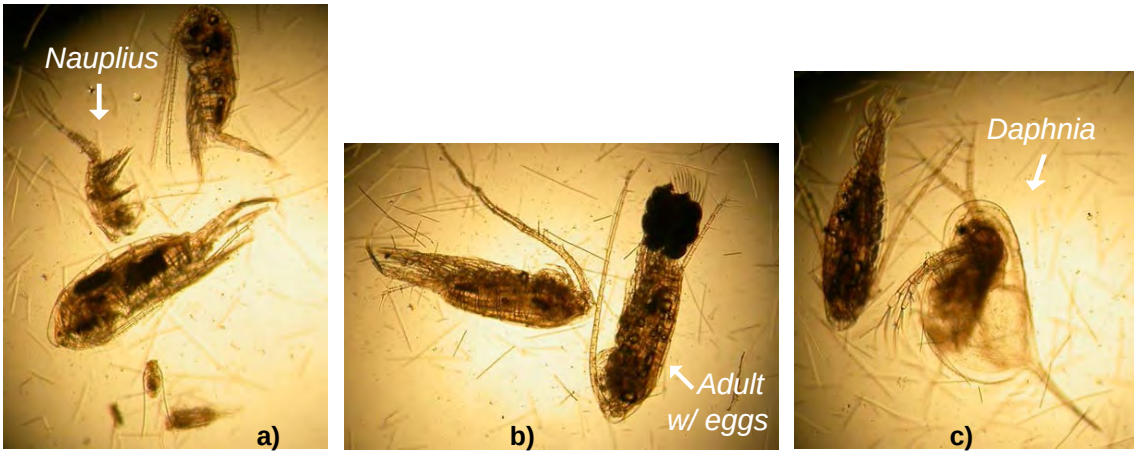

Fig. 1. Images of zooplankton in Lake Elsinore: a) adult copepods and nauplius; b) adult copepods, including reproductive adult; c) the single Daphnia present in samples. Filaments are Pseudanabaena.

This low proportion of *Daphnia* within the zooplankton community is consistent with findings from 2003-4 and 2009-10 when cladocerans comprised <0.6% of the community (Anderson et al., 2011). High TDS and/or high threadfin shad populations are thought to be responsible (Veiga-Nascimento, 2005).

Fishery

The hydroacoustic survey was conducted along the 7 transverse transects as in previous surveys (Fig. 2). The short longitudinal transect in the southern end of the lake was not surveyed due to the very shallow depth over most of the transect.

Fig. 2. Hydroacoustic survey transects.

Aggregating the transect data, population estimates were determined for 16 acoustic size classes from -30 to -70 dB (2.5 dB/bin) (Fig. 3). Love's equation (Love, 1970) was used to estimate fish length (Fig. 3, upper x-axis) from the acoustic target strength (Fig. 3, lower x-axis) as done in previous surveys (eq 1):

$$TS = 19.1 \log L - 0.9 \log F - 62.0 \quad (1)$$

where *TS* is the target strength (dB) and *F* is the echosounder acoustic frequency (kHz). As noted in Anderson et al. (2011), these length estimates are thought to be biased low based upon paired hydroacoustic and gill net measurements, but are retained here for comparison with other reported values and survey results. One sees that numerical abundance of fish in Lake Elsinore are dominated by small fish <3.5 cm in length (Fig. 3). These small fish comprise 95.6% of the total number of fish targets identified in the survey and are estimated to be present at an areal density of approximately 54,100 fish/acre. This approximate size class (1-3.5 cm) is consistent with threadfin shad, which are thought to dominate the fishery. In contrast, the population density for fish >20 cm in length is estimated to be 12.3 fish/acre.

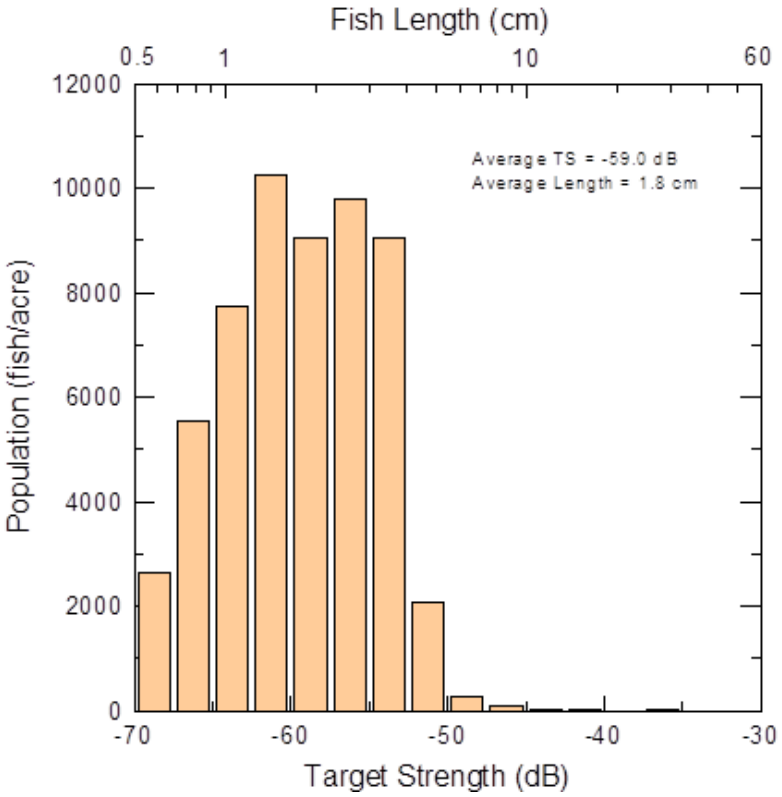

Fig. 3. Population estimates (fish/acre) vs. target strength (dB) (lower x-axis) and approximate fish length based upon Love's equation (upper x-axis).

The results from this survey can be compared with other hydroacoustic surveys conducted at the lake (Table 2). The April 24, 2008 survey yielded a population estimate of 18,090 fish/acre with a mean size of 4.7 cm. Fish >20 cm, which would principally represent piscivores and carp, number 1,050 fish/acre and comprise 5.8% of the entire fish population. The survey conducted following the fish kill in the summer of 2009 found dramatically reduced total population (2,2867 fish/acre) with slightly lower mean size that found in April 2008 (Table 2). Density of fish >20 cm was only 6/acre and constituted only 0.2% of the total population. Populations had rebounded quickly by December 1, 2010, reaching 27,720 fish/acre with a mean size of 4.3 cm; abundance of fish >20 cm in length increased slower, but did reach 273 fish/acre and 1.0% of the total population.

Table 2. Fish survey results comparing current survey (April 2, 2015) with surveys conducted in 2008 and 2010.

Date	Population (fish/acre)	Mean Size[a] (cm)	Size Range[a] (cm)	Fish >20 cm[a] (fish/acre)
April 24, 2008	18,090	4.7	0.5 - 100	1,050 (5.8%)
March 15, 2010[b]	2,867	4.0	0.5 – 29	6 (0.2%)
December 1, 2010	27,720	4.3	0.5 – 61	273 (1.0%)
April 2, 2015	56,600	1.8	0.5 - 30	12 (0.02%)

[a]*Based on Loves' equation.*
[b]*March 15, 2010 survey was conducted after fish kill in summer of 2009.*

The present survey, conducted on April 2, 2015, found the largest population of fish in the lake (56,600 fish/acre), although the fish were much smaller in size than in other surveys (mean length of 1.8 cm) (Table 2). Moreover, very few fish larger fish (>20 cm) were present at the time of this survey. As previously noted, the TDS at the time of this survey was the highest at any time since regular monitoring began at the lake, and values were markedly higher than observed in 2008 and 2010. Threadfin shad are tolerant of salinities as high as 15,000 mg/L; in contrast, black crappie have a maximum salinity tolerance of about 2,000 mg/L. Black crappie were the dominant piscivore present in Lake Elsinore in 2006-2007 based upon beach seine observations during carp removal efforts at the lake, but are thought to be effectively absent in 2015. Largemouth bass can tolerate higher salinities than black crappie, although literature suggests reproduction and recruitment can be impaired at TDS values greater that about 2,000-2,500 mg/L.

Based upon these findings, the lake in spring 2015 was in very poor ecological condition, with a very large amount of *Pseudanabaena*, limited capacity for zooplankton grazing of phytoplankton, and susceptible to a large fish kill. A modest fish kill was observed beginning August 4, 2015.

Conclusions

The results of these ecological measurements made at Lake Elsinore in spring 2015 indicate:

(i) very poor water quality, with TDS at levels not seen at the lake since regular monitoring began in 2000, and Secchi depth values <10-15 cm;

(ii) a zooplankton community dominated by copepods and nauplii, with negligible numbers of rotifers and a single Daphnia identified in samples;

(iii) an ecologically unsustainable fishery, with a very large number of small threadfin shad and low relative number of larger fish;

(iv) the subsequent fish kill in the summer of 2015 may have helped rebalance the fishery and food web in the lake, although reduction in the TDS concentration and inundation of shoreline vegetation providing new habitat is thought to provide greater ecological value.

References

Anderson, M.A. 2008. *Hydroacoustic Fisheries Survey for Lake Elsinore: Spring, 2008.* Draft Final Report to the City of Lake Elsinore. 15 pp.

Anderson, M.A., J. Tobin and M. Tobin. 2011. *Biological Monitoring for Lake Elsinore.* Final Report to the Lake Elsinore-San Jacinto Watershed Authority. 57 pp.

Love, R.H. 1970. Dorsal-aspect target strength of an individual fish. *J. Acoust. Soc. Am.* 49:816-823.

Technical Memorandum

Task 2.3: Bathymetric Survey and Sediment Hydroacoustic Study of Canyon Lake

Objectives

The overall objective of this task was to better understand the basin characteristics of Canyon Lake. Specific objectives were to:

- Develop up-to-date bathymetric map
- Derive up-to-date storage curve for the reservoir
- Estimate volume of sediment deposited and its distribution
- Characterize distribution of sediment properties across the basin

Approach

A hydroacoustic survey was conducted at Canyon Lake over 2-days on December 16-17, 2014. The survey was conducted using a BioSonics DTX echosounder with multiplexed 38- and 430-kHz single beam transducers with integrated pitch-roll sensors and a 201-kHz split beam transducer (Table 1). Transducers were operated at 5 pps on each frequency, with 0.4 ms pulse duration. Transducers were mounted 0.5 m below the water surface with position recorded using a JRC 202W real-time differential GPS. Data were acquired using BioSonics VisualAcquisition v.6.0 software on a Dell ATG laptop. Calibrations were conducted each day using tungsten carbide spheres of known target strength. Data files were processed using BioSonics VBT software.

Table 1. Transducer configurations used in this study.

Property	DTX-38	DTX-200	DTX-420
Frequency (kHz)	38	201	430
Beam angle (°)	10.0	6.6	7.0
Source level (dB μPa^{-1})	217.0	221.3	220.0
Receive sensitivity (dbC μPa^{-1})	-41.1	-57.6	-62.9
Pulse length (ms)	0.4	0.4	0.4
Pings per second (pps)	5	5	5

Water column and sediments were also sampled. Water temperature and conductivity profiles were measured daily with an YSI CastAway CTD. Bottom sediments were sampled with an Ekman dredge at 5 sites across the lake, homogenized and subsampled into 500-mL widemouth glass jars with Teflon lined screw top lids, and returned to the lab for basic characterization. Phosphorus in bottom sediments of lakes exists in numerous forms, including a mobile form (mobile-P) that includes soluble/exchangeable forms as well as that associated with iron (Fe)(III) phases that can be released upon reduction of Fe(III) under low dissolved oxygen (DO) conditions (Reitzel et al., 2005; Pilgrim et al., 2007). Mobile-P in surficial sediments has been shown to be strongly correlated with internal recycling rates (Pilgrim et al., 2007), with

the mobile-P pool reduced by amounts consistent with that released to the water column (Reitzel et al., 2005).

Sediment grab samples were subsampled for dry-weight determination and extracted for mobile-P following Pilgrim et al. (2007). Water content was determined on subsamples that were heated overnight at 105 °C. Total C and N were measured by dry-combustion methods using a Thermo Flash EA NC soil analyzer (Nelson and Sommers, 1982). Inorganic C and $CaCO_3$ were determined manometrically following Loeppert and Suarez (1996), with organic C taken as the difference between total C and inorganic C. Duplicate analyses were conducted at a rate of at least one every 10 samples within an analytical batch.

Results

Bathymetry

Depth varied widely across the lake, with predictably greatest values located near the dam in the main basin of the lake, exceeding 17 m at full pool (Fig. 1). The north and east basins possessed lower depths, with less than about 11 m in the east basin near the causeway, and less than about 7 m throughout the north basin (Fig. 1).

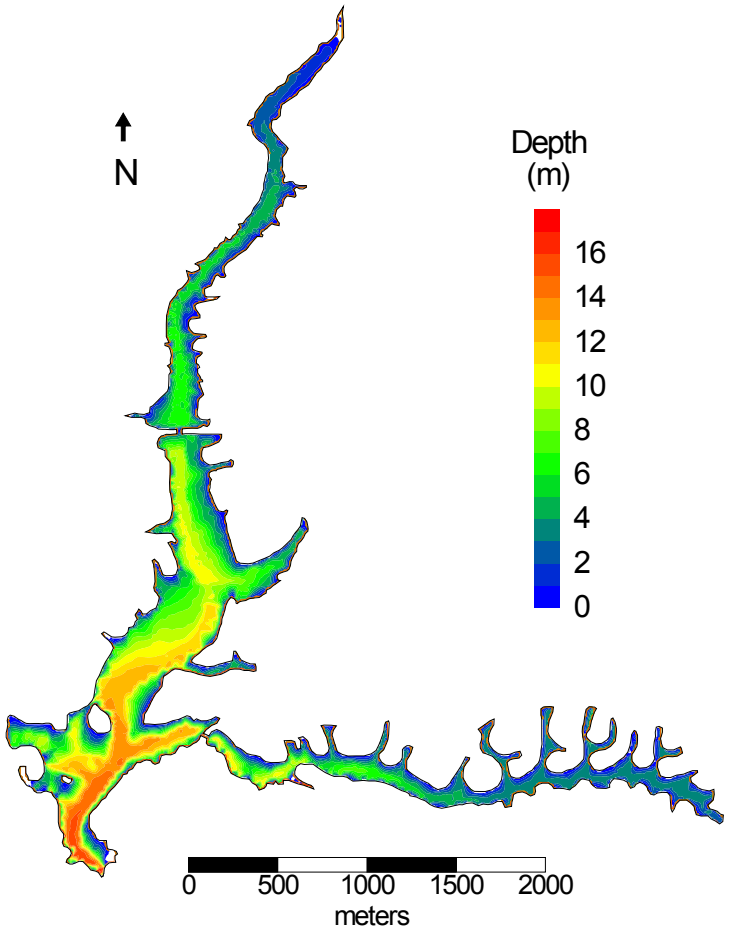

Fig. 1. Bathymetry of Canyon Lake.

Very shallow conditions were present near the inflows of the San Jacinto River and Salt Creek, reflecting natural topography and the deposition of material eroded from the watershed. Bathymetric measurements also revealed the original channel for the San Jacinto River which was located on the western side of the lake through the north basin and into the main basin (Fig. 1). The channel was not clearly defined near the mid-portion of the main basin due presumably to deposition of material there, likely derived from construction activities during development of the community. The channel is again evident in the southern part of the lake, representing its deepest region (Fig. 1).

The bathymetric data were used to develop an up-to-date storage curve and elevation-area curve for the lake (Fig. 2). Included is storage curve provided by EVMWD (Fig. 2a, dashed line). The interpolation assumed the shoreline throughout the north basin and most of the main basin to grade to 0 m at full pool, while the shoreline of east basin was defined by sea walls with an assumed depth of 0.6 m. The basin elevation ranged from a minimum value of 1323.36 ft (above MSL), immediately adjacent to the dam face, to the spillway elevation of 1381.76 ft. The full pool volume of Canyon Lake was calculated to be 8758 acre-feet, a value that is 3110 acre-feet less than EVMWD's prior storage curve apparently developed in 1993. The downward displacement of lake volume at a given surface elevation represents loss of storage; measurements thus indicate that the lake has lost significant storage over time.

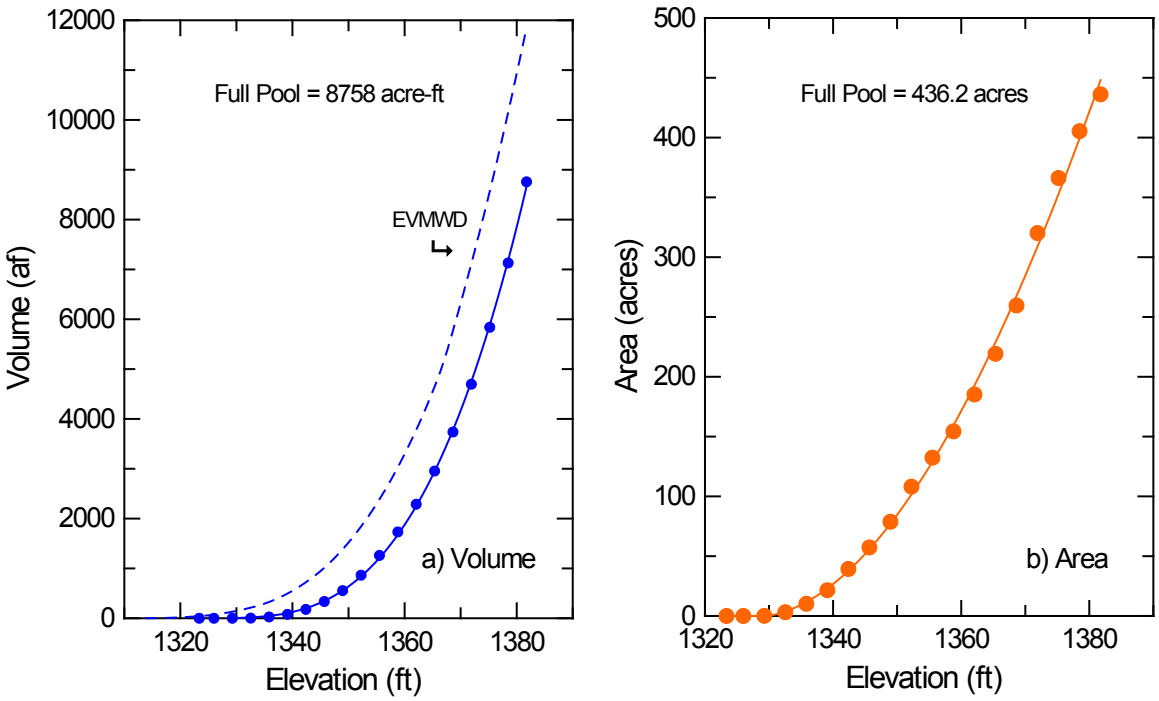

Fig. 2. Canyon Lake hypsography: a) volume vs. elevation (dashed line is EVMWD data from 1993), and b) surface area vs. elevation.

The lake volume was well-fit (r^2=0.9998) by the 3rd-order polynomial of the form:

$$Vol\ (af) = -129913027.7 + 293417.3*Elev - 220.9033*Elev^2 + 0.0554373*Elev^3 \quad (1)$$

The surface area at full pool was calculated to be 436.2 acres (Fig. 2b). Lake surface area was reasonably described (r^2=0.9980) with the 3rd-order polynomial:

$$Area\ (acres) = 1271585.1 - 2645.223*Elev + 1.82046*Elev^2 - 0.00041385*Elev^3 \quad (2)$$

In addition, the elevation-area-volume relations for the individual basins were also developed. The main basin contributes the largest area and volume to the lake, at 252.8 acres and 6439.8 acre-feet, representing 58.0% of the total area and 73.5 % of the total volume, respectively (Table 1). The east and north basins collectively comprise over 40% of the lake area, but contribute only about 25% of the total lake volume (at full pool) (Table 2).

Table 2. Individual basin and total lake metrics.

	Area (acres)	Volume (acre-ft)	Mean Depth (ft)	Maximum Depth (ft)
Main Basin	252.8 (58.0%)	6439.8 (73.5%)	25.5	58.4
East Basin	102.5 (23.5%)	1406.8 (16.1%)	13.78	38.7
North Basin	80.9 (18.5%)	911.2 (10.4%)	11.3	26.2
Total	436.2 (100%)	8757.9 (100%)	20.1	58.4

Storage curves for individual basins were also extracted from bathymetric data (Fig. 3).

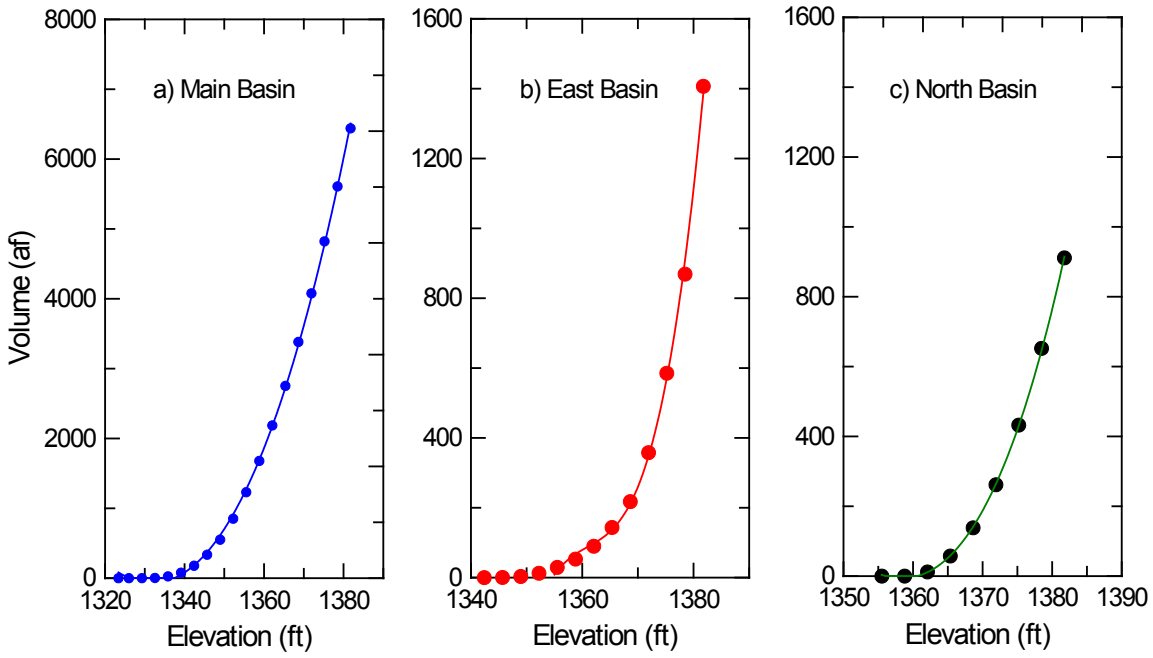

Fig. 3. Volume-elevation relationships for a) main basin, b) east basin and c) north basin.

The volumes of the individual basins were also reasonably-described (r^2>0.998) by 3rd-order polynomials:

$$Vol_{main} = -18099718.1 + 43668.02*Elev - 34.9638*Elev^2 + 0.0092954*Elev^3 \quad (3)$$

$$Vol_{east} = -312755907.3 + 689395.0*Elev - 506.541*Elev^2 + 0.1240641*Elev^3 \quad (4)$$

$$Vol_{north} = -50991062.6 + 114231.5*Elev - 85.2843*E*Elev^2 + 0.0212201*Elev^3 \quad (5)$$

Sediment Thickness

Thickness of the sediment was derived from echograms based upon the penetration and attenuation of the 38-kHz sound wave within the sediments. Very hard sediments limit penetration of the sound wave, while fine-textured organic-rich sediments with high water contents allow penetration of the sound wave to considerable depths within the sediments before reverberation from harder weathered bedrock or soil. Thickness of the sediment ranged from 0 – 8 m, and varied across the basin in a complex way, with some evidence of infilling of the original San Jacinto River and Salt Creek channels, deposition of material derived from grading and construction within the local watershed and from erosion from upper watersheds (Fig. 4).

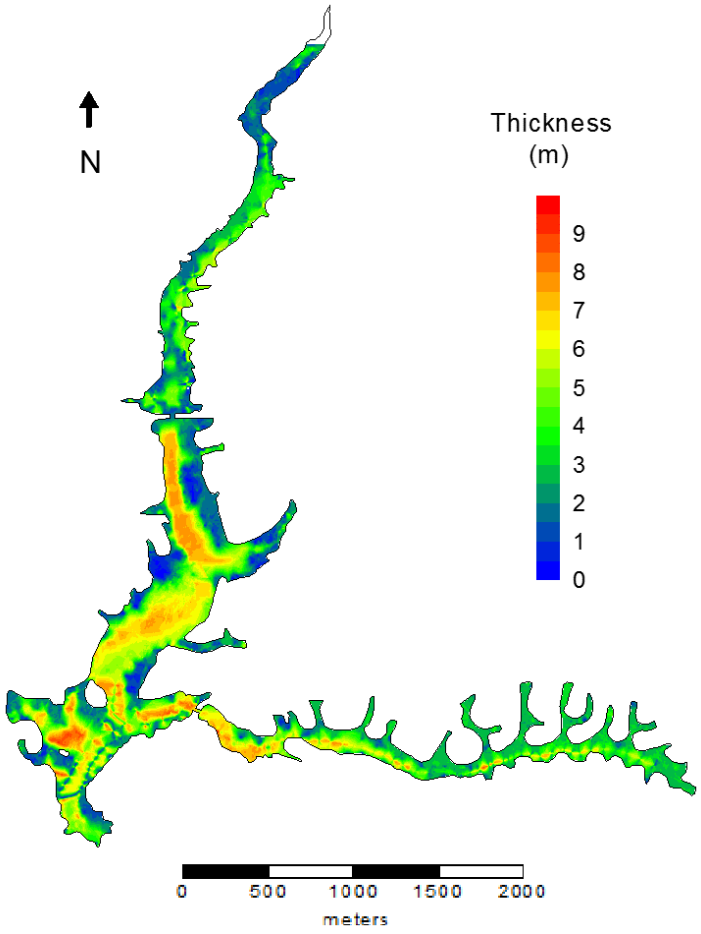

Fig. 4. Sediment thickness in Canyon Lake.

Based upon these measurements, it is estimated that sedimentation over the past 88 yrs since the dam was constructed has reduced the capacity of the reservoir by >5000 acre-feet and potentially as much as 8000 acre-feet or more.

Sediment Organic C Content

The attributes of the bottom echo have been found to be correlated with surficial sediment physical and chemical properties (Anderson and Pacheco, 2011). For example the fractal (box) dimension of the bottom echo at 430-kHz was very strongly correlated with the organic C content of surficial bottom sediments. The regression equation developed in that study was used to estimate the organic C content of sediments in Canyon Lake (Fig. 5).

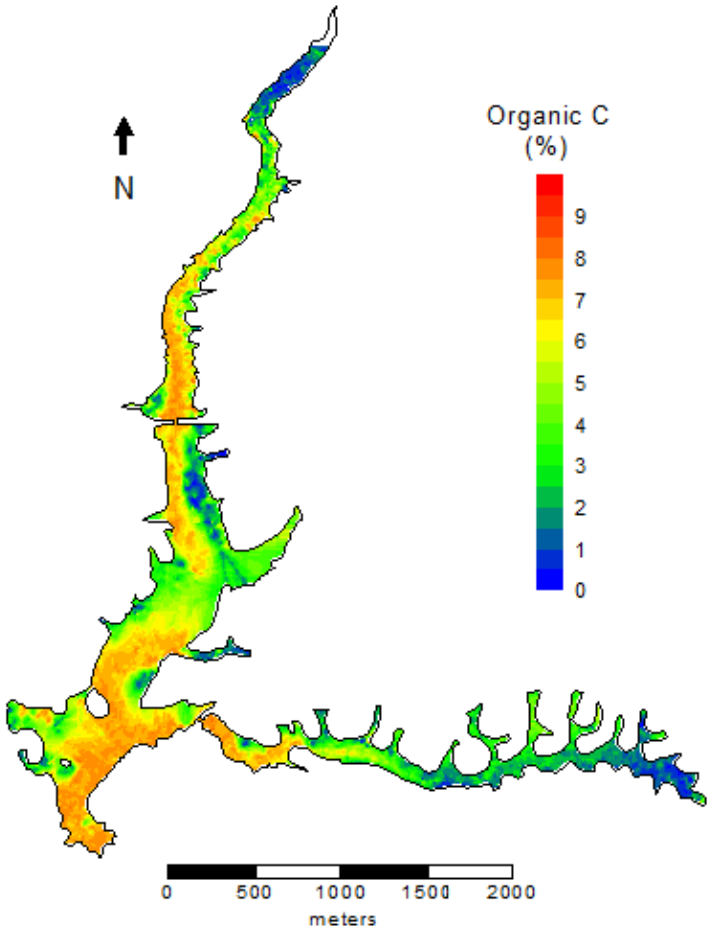

Fig. 5. Sediment organic C content in Canyon Lake.

Organic C contents of surficial sediments were very low near the influent of San Jacinto River and Salt Creek (<1%) as a result of deposition of coarse-textured material

eroded from the watershed, and due to scouring and further transport of finer-textured material during inflow events. Organic C contents increased at greater distances into east and north basins, with strong focusing of organic matter in the deeper waters of the main basin, especially near the dam (Fig. 5).

Sediment Mobile-P Content

The mobile-P content of sediments has been found to be strongly correlated with P flux from sediments under low DO conditions and is now commonly used to guide alum treatments of lakes. Mobile-P was quanitifed on sediment grab samples from 5 sites on the lake when hydroacoustic measurements were also conducted. A nonlinear relationship was found between the fractal dimension of the bottom echo envelope and mobile-P content (Fig. 6).

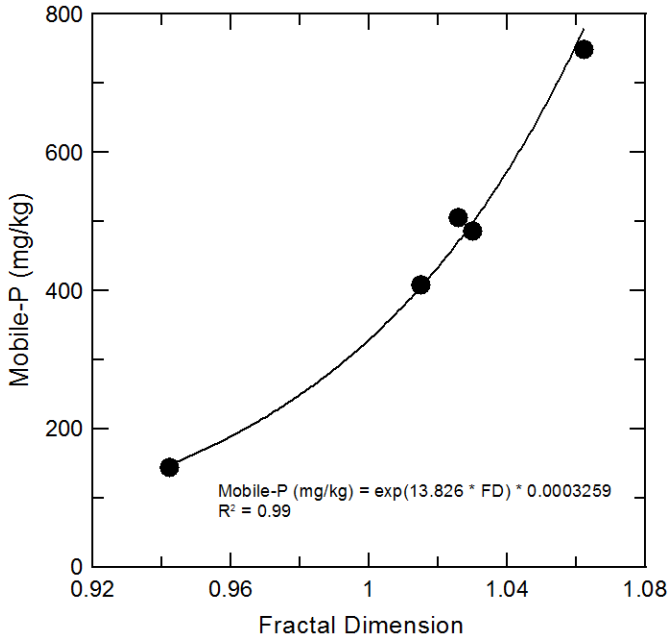

Fig. 6. Mobile-P content in surficial sediment vs. fractal dimension of bottom echo at 430-kHz.

This allowed us to remotely sense mobile-P content of sediments and to develop a map of its distribution across the lake (Fig. 7). Mobile-P content of surficial sediments was enriched in original river channel in the north basin; mobile-P was also elevated in deeper sediments near closer to dam (Fig. 7). Understanding of the distribution of mobile-P helps guide alum treatment for sediment P inactivation. Thus, alum treatments designed to inactivate mobile-P in the main basin sediments of Canyon Lake would be most effective when targeting the large inventories at the southern end of the lake. The

limited exchange between basins during most of the year (excluding large runoff and flushing events) requires that each basin be treated essentially as an independent lake.

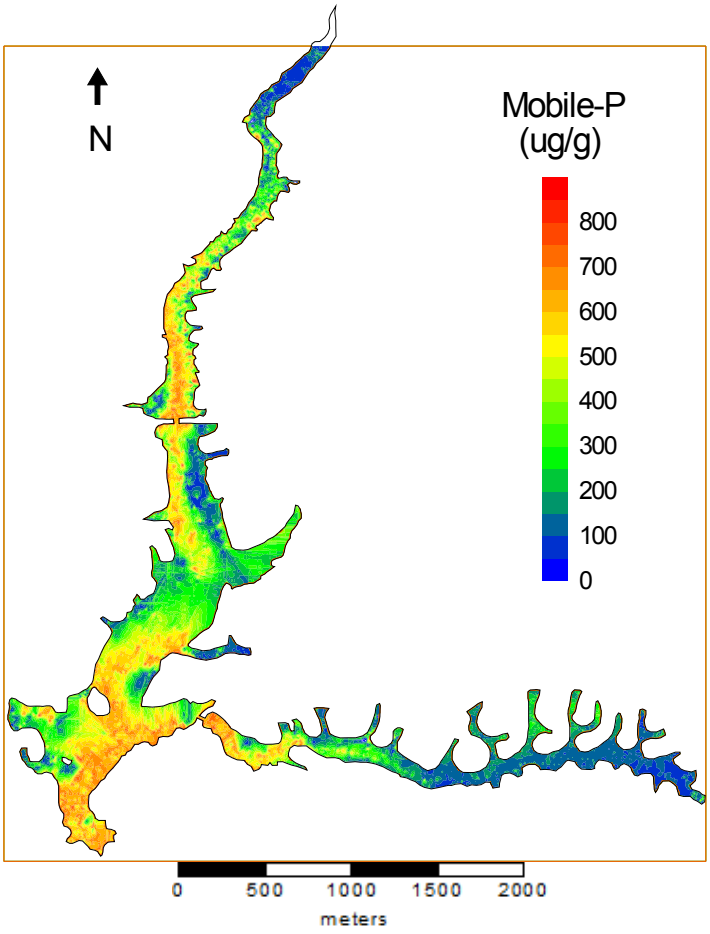

Fig. 7. Sediment mobile-P content in Canyon Lake.

Conclusions

The hydroacoustic study provided valuable new insights in the characteristics of Canyon Lake:

- The hydroacoustic survey provides up to date bathymetry and elevation-area-volume relations for Canyon Lake
- Measurements also provided new detailed understanding of the distribution, properties and thickness of sediment within the lake
- Sedimentation is projected to have reduced storage capacity by >5000 acre-feet and potentially as much as 8000 acre-feet or more since dam construction in 1927

- Sediments enriched in mobile-P and organic matter were deposited in deeper regions of lake, and represent regions of greater nutrient flux and oxygen demand

References

Anderson, M.A. and P. Pacheco. 2011. Characterization of bottom sediments in lakes using hydroacoustic methods and comparison with laboratory measurements. *Water Res.* 45: 4399-4408.

Loeppert, R.H. and D.L. Suarez. 1996. Carbonate and gypsum. In: Sparks, DL, editor. *Methods of Soil Analysis. Part 3.* 3rd ed. Agronomy Monographs 9. ASA and SSSA. Madison, WI. pp. 437-474.

Nelson, D.W. and L.E. Sommers. 1982. Total carbon, organic carbon, and organic matter. In: A.L. Page, R.H. Miller, and D.R. Keeney, editors *Methods of Soil Analysis, Part 2*. 2nd ed. Agronomy Monographs 9. ASA and SSSA., Madison, WI. pp. 539-580.

Pilgrim, K.M., B.J. Huser and P.L. Brezonik. 2007. A method for comparative evaluation of whole-lake and inflow alum treatment. *Water Res.* 41:1215-1224.

Reitzel, K., J. Hansen, J., F. Ø. Andersen, K.S. Hansen, and H.S. Jensen. 2005. Lake restoration by dosing aluminum relative to mobile posphorus in the sediment. *Environ. Sci. Technol.* 39: 4134–4140.

Technical Memorandum

Task 2.4: Mobile-P and Internal Phosphorus Recycling Rates in Canyon Lake

Objective

The objective of this task was to improve understanding of phosphorus biogeochemistry in Canyon Lake sediments and the factors affecting P recycling through measurements of mobile-P contents and internal recycling rates of sediments.

Approach

Measurements of mobile-P, Al-P and internal P recycling rates in Canyon Lake were conducted to assess progress made by alum additions in sequestering bioavailable/mobile-P. Mobile-P and Al-P contents of sediments were determined on grab samples and cores collected from the 5 sites previously sampled for water quality and nutrient flux measurements (Fig. 1) following Pilgrim et al. (2007). In additional P flux measurements were made on triplicated intact sediment cores following Anderson (2001).

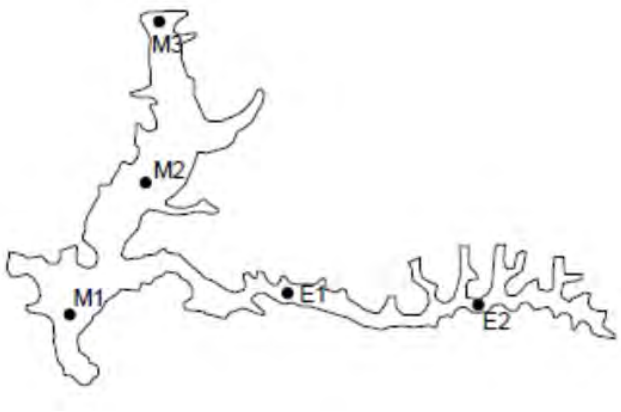

Fig. 1. Sampling sites on Canyon Lake.

An Ekman dredge was used to collect a grab sample, which was then subsampled by carefully inserting a 30.5 cm by 6.3 cm diameter Lucite tube approximately 10 cm into the sediment. The bottom of the core was sealed using a rubber stopper. The core was then carefully topped off with bottom water sampled using a van Dorn sampler, stoppered with zero headspace and transported back to the lab.

Cores were then incubated in the dark at the temperature and DO levels measured at the time of sampling. Approximately 10 mL of water were removed daily, filtered and analyzed for soluble PO_4-P using a Seal discrete analyzer following standard methods (APHA, 1989). Dissolved oxygen concentrations were measured using a YSI Model 55 DO meter, with the water briefly sparged with N_2 or lab air as needed to maintain DO and to very gently mix the water column within the core. The measured

change in concentration was used in conjunction with water volume and sediment-water interfacial area to calculate nutrient flux rates and compared with previously measured values.

Results

P Internal Recycling Rates

The flux of PO_4-P from bottom sediments sampled in August 2014 was lower at 4 out of 5 sites compared with average values measured in 2001, 2002 and 2006 (Fig. 2).

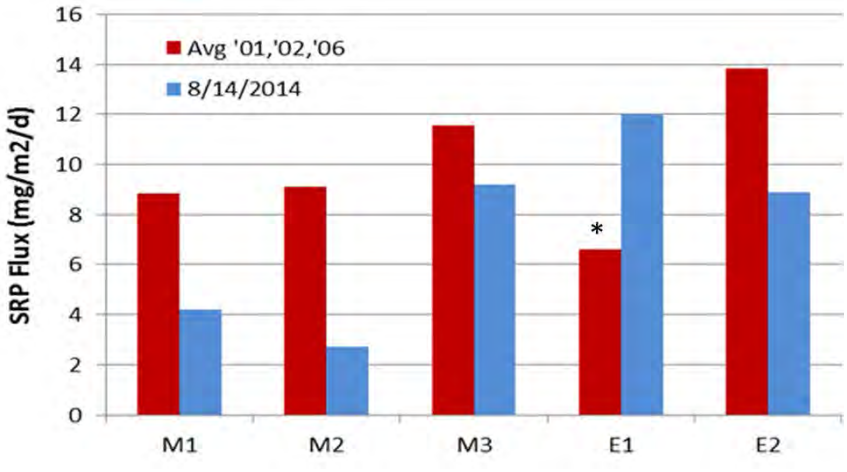

*Fig. 2. PO_4-P flux rates measured at the 5 sampling station comparing the average values from 2001, 2002 and 2006 with rates measured on August 14, 2014. *Data available only for 2006 at site E1.*

Average values do obscure strong inter-annual variability, however. In particular, the very large runoff events in 2005 increased subsequent PO_4-P flux rates at sites M1 and E2 (Fig. 3). If we ignore the 2006 data and its impact on average values, alum treatments in F'13 and W'14 appear to have had more modest and variable impacts on PO_4-P flux (Fig. 3). Inter-annual variability in rate of sediment release of PO_4-P makes it difficult to draw conclusions about effects of alum applications on P recycling from sediments as of the time of these measurements. It is thought that speciation of P within the sediments may provide a more sensitive measure of alum effects; moreover, mobile-P measurements are increasingly used to design alum treatment projects and determine appropriate alum application rates (Pilgrim et al., 2007).

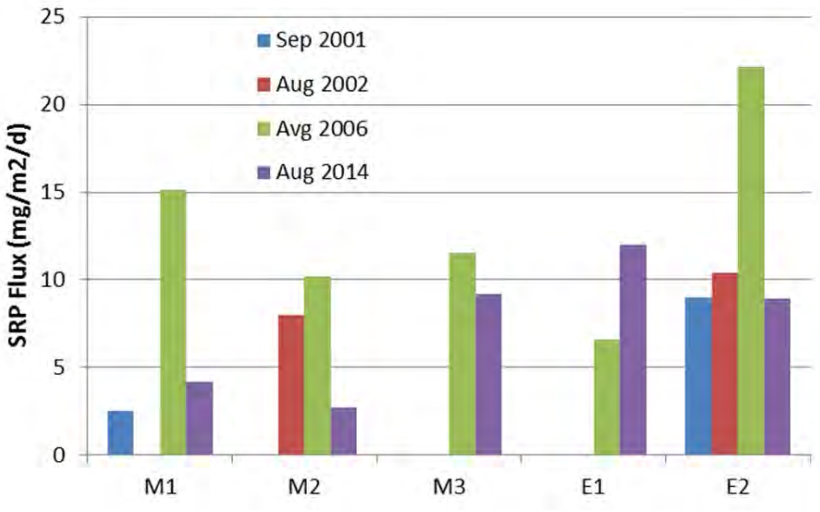

Fig. 3. Summer PO_4-P flux rates from intact cores collected from Canyon Lake.

Mobile-P and Al-P Contents

Mobile-P contents in sediments of Canyon Lake were markedly higher than concentrations recently measured in Lake Elsinore and Big Bear Lake (Fig. 4). The concentration at site M1 was 749 µg/g, a value nearly 4x larger than the highest concentration measured at Lake Elsinore and 2.8x higher than the highest concentration in Big Bear Lake (Fig. 4). Concentrations of mobile-P at sites M2, M3 and E1 were 409 – 506 µg/g, while site E2 in East Bay was 145 µg/g.

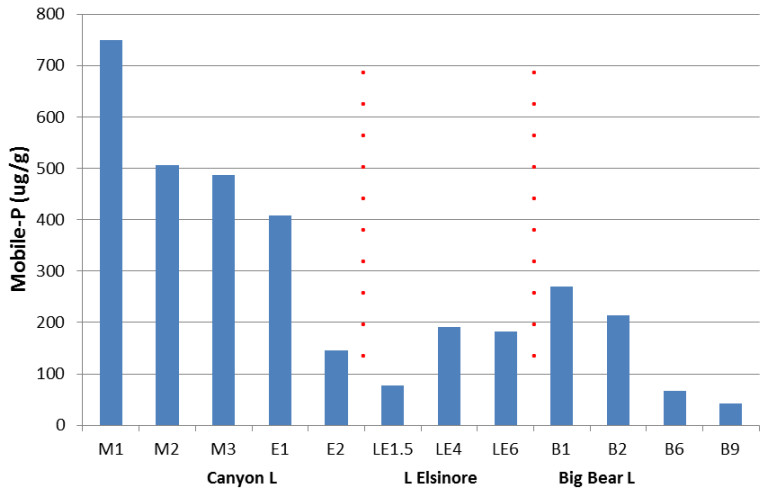

Fig. 4. Mobile-P content (µg/g) of sediment samples collected from Canyon Lake, Lake Elsinore and Big Bear Lake.

Mobile-P is generally better expressed on an areal basis since it better correlates with flux rates and allows for calculation of alum dose. Assuming a reactive depth of 10

cm, the range of mobile-P contents is reduced among the 3 lakes, but Canyon Lake is still consistently the highest at an average concentration of 6.68 g mobile-P/m^2 (Fig. 5).

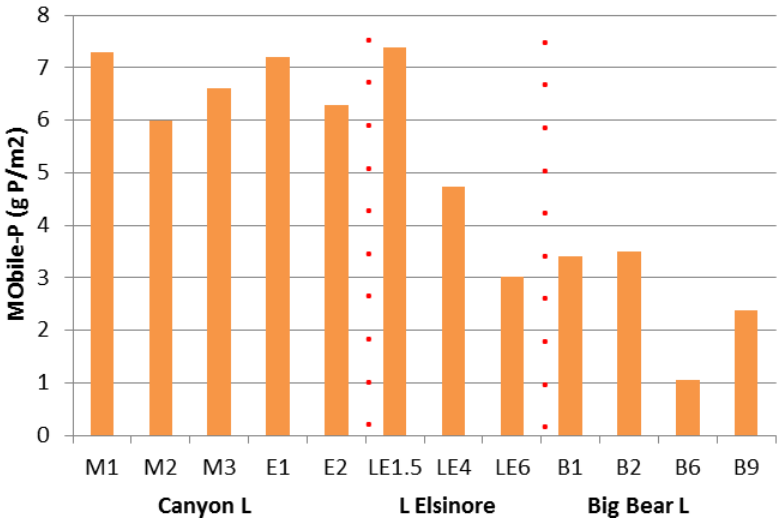

Fig. 5. Mobile-P content, expressed on areal basis (g P/m^2), of sediment samples collected from Canyon Lake, Lake Elsinore and Big Bear Lake.

Assuming a 20:1 Al:P ratio for the alum floc (Berkowitz et al, 2006), the mobile-P pool in the sediments of Canyon Lake may require up to 140 g Al/m^2, an average value much higher than that for Lake Elsinore or Big Bear Lake, although comparably high application rates would be needed for some regions on Lake Elsinore (Fig. 6).

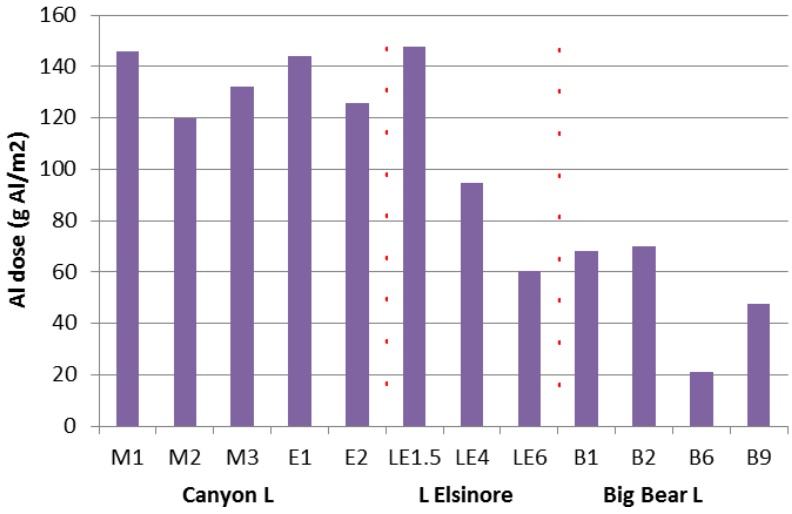

Fig. 6. Alum dose, expressed as g Al/m^2, based upon mobile-P values assuming 20:1 Al:P ratio.

The hydroacoustic survey conducted on Canyon Lake in December 2014 (Task 2.3) quantified the acoustic properties of bottom sediments as well as bathymetry. The

fractal dimension of the bottom echo envelope was strongly correlated with mobile-P content of bottom sediments (Fig. 7), allowing development of a map showing mobile-P distribution across the lake (Fig. 8, previously presented in the Task 2.3 tech memo).

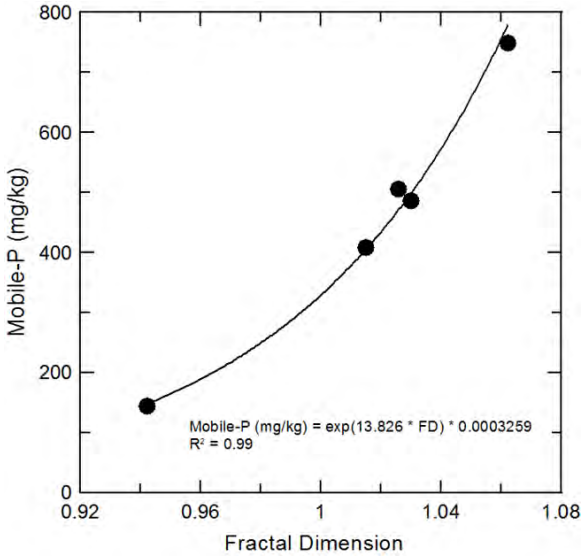

Fig. 7. Mobile-P content of Canyon Lake sediment vs fractal dimension of bottom echo envelope.

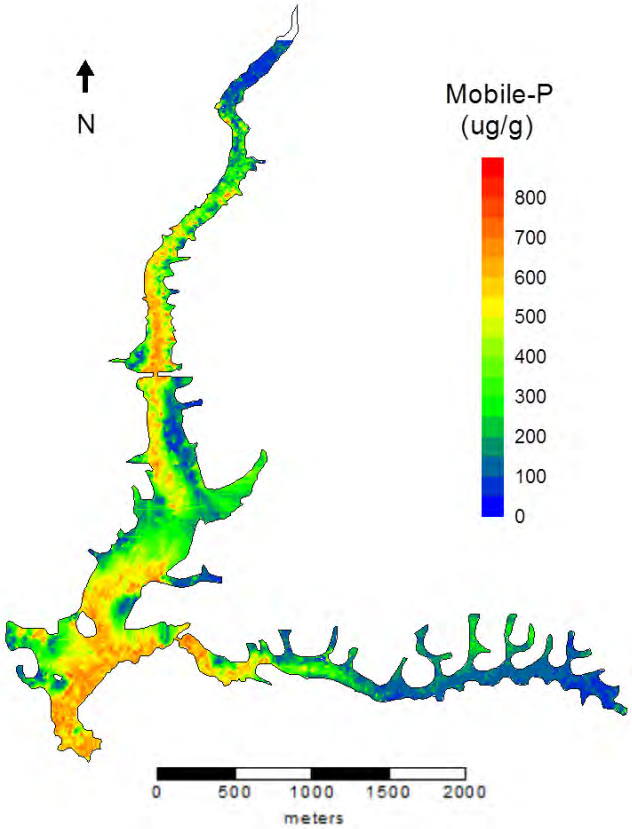

Fig. 8. Distribution of mobile-P in bottom sediments of Canyon Lake.

The results presented above were based upon grab samples collected using an Ekman dredge that samples to approximately 10-15 cm depth in soft cohesive sediments and less in coarser textured uncohesive material. Intact sediment cores were also collected from each of the 5 sampling sites on Canyon Lake and sectioned into 1 cm increments that were subsequently extracted for mobile-P and Al-P (Fig. 9).

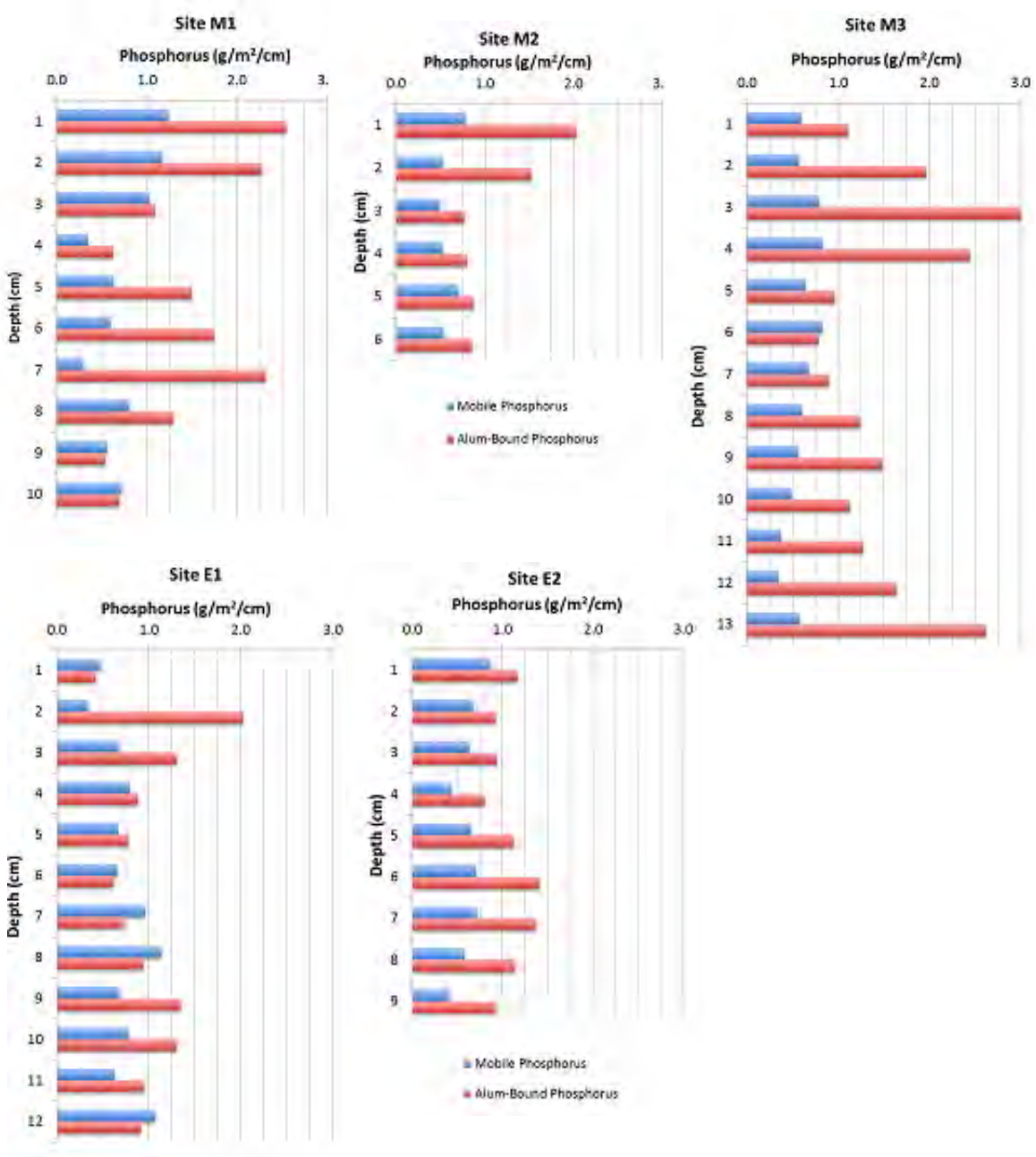

Fig. 9. Vertical distribution of mobile-P and Al-P in sediments of Canyon Lake.

Phosphorus extracted with NaOH and assigned to the aluminum-bound pool (that would include P bound to both natural Al phases as well as added alum) (Fig. 9, red bars) typically exceeded concentrations of mobile-P, often by a relatively wide margin (Fig. 9 blue bars), although clear vertical trends across the sites are not apparent. Ideally, a reduction in mobile-P and a corresponding increase in Al-P would result from an alum treatment and signify the conversion of labile forms of P to unreactive forms. The 7 cm depth at site M1 might be conjectured to conform to this, but would require added alum floc to have settled to this depth within the sediments in a relatively narrow band. Watershed inputs of inorganic particles with large runoff events, intervals of drought, and other processes would also be expected to alter properties with depth.

Despite this complexity, it is interesting to compare P fractionation results from sediment samples collected in December 2006 (Whiteford et al., 2007), following the tremendous runoff and siltation to Canyon Lake from winter 2005 storms, with results in this study (Fig. 10). The results for 2014 and 2006 are presented side-by-side as stacked bar charts for the NH_4Cl-P, Fe-P and Al-P fractions, with sites separated from each other by dashed lines. Soluble and readily exchangeable P (NH_4Cl-P) comprised a small fraction of P in the sediments in both 2006 and 2014 (Fig. 10, dark red bar), while Fe-P comprised a much larger fraction (Fig. 10, pale blue bar). The sum of these 2 phases is taken as mobile-P; what is clear is the Fe-P and mobile-P contents were much higher at all sites in 2006 when compared with 2014 (Fig. 10). Encouragingly, Al-P contents were often quite a bit higher in 2014 than 2006, potentially indicating the alum treatments had some success in lowering mobile-P and increasing the fraction bound to Al.

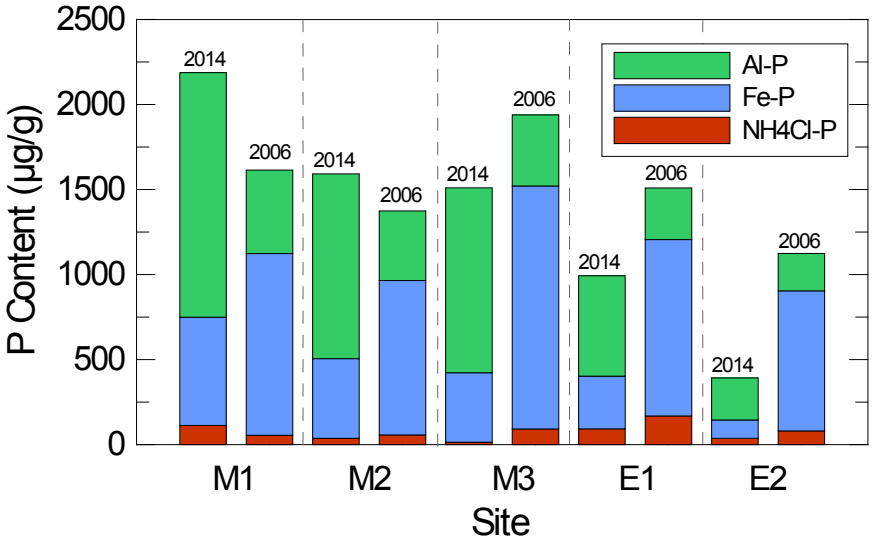

Fig. 10. Phosphorus fractionation in sediments of Canyon Lake comparing results from samples collected in this study with those from 2006 (Whiteford et al., 2007).

There are interesting lake management implications from the P fractionation results for Canyon Lake and Lake Elsinore. The differences between these 2 lakes can be attributed in part to the San Jacinto River that delivers a substantial amount of inorganic particulate material, eroded from the watershed, which is retained within Canyon Lake. As a result, Canyon Lake has much higher mobile-P contents, chiefly as Fe-P, than Lake Elsinore (Task 2.1 Tech Memo). With high reducible Fe-bound P phases in Canyon Lake, Canyon Lake would likely be more responsive to aeration/ oxygenation than Lake Elsinore. The limited amount of Fe delivered to Lake Elsinore, and the previously established formation of FeS_2(s) phases within the sediments (Anderson, 2001) is thought to constrain effectiveness of aeration at sequestering sediment PO_4-P there.

Conclusions

The results of these measurements indicate:

(i) Canyon Lake has much higher mobile-P contents than Lake Elsinore and Big Bear Lake;

(ii) the mobile-P pool in Canyon Lake is chiefly comprised of PO_4-P associated with reducible Fe phases (Fe-P), making it more amenable to aeration/oxygenation for sequestering PO4-P within the sediments than Lake Elsinore with very little Fe-P.

(iii) mobile-P concentrations are generally much higher in deeper regions of the lake as a result of sediment focusing processes;

(ii) P fractionation results indicate a reduction in mobile-P and increase in Al-P contents since 2006 in Canyon Lake that may result from differences in hydrologic conditions, alum applications, or other factors.

References

Anderson, M.A. 2001. *Internal Loading and Nutrient Cycling in Lake Elsinore.* Final Report to the Santa Ana Regional Water Quality Control Board. 52 pp.

Berkowitz, J., M.A. Anderson and C. Amrhein. 2006. Influence of aging on phosphorus sorption to alum floc in lake water. *Water Res.* 40:911-916.

Boudreau, S. and M.A. Anderson, 2016. *Task 2.1: Stable Isotope, Elemental and Mobile-P Measurements in Lake Elsinore Sediments.* Technical Memorandum the Lake Elsinore & Canyon Lake TMDL Task Force. 24 pp.

Pilgrim, K.M., B.J. Huser and P.L. Brezonik. 2007. A method for comparative evaluation of whole-lake and inflow alum treatment. *Water Res.* 41:1215-1224.

Whiteford, J., C. Paez and M. Anderson. 2007. *Sediment Nutrient Flux and Oxygen Demand Study for Canyon Lake with Nutrient Monitoring and Assessment of In-Lake Alternatives: January-March 2007.* Draft Report to LESJWA. 15 pp.